

Back in bismuth: Controlling triplet energy transfer, phosphorescence, and radioluminescence via supramolecular interactions

Alexander C. Marwitz,¹ Aaron D. Nicholas,² Rajani Thapa Magar,⁴ Anuj K. Dutta,¹ Joel Swanson,¹ Tyler Hartman,¹ Jeffery A. Bertke,¹ Jeffrey J. Rack,⁴ Luiz G. Jacobsohn,³ Karah E. Knope^{1,*}

1 Department of Chemistry, Georgetown University, Washington, D.C. 20057, United States of America

2 National Security Directorate, Pacific Northwest National Laboratory, 902 Battelle Boulevard, Richland, WA 99354, United States of America

3 Department of Materials Science and Engineering, Clemson University, Clemson, SC 29634, United States of America

4 Department of Chemistry and Chemical Biology, University of New Mexico, Albuquerque, NM 87111, United States of America

Supporting Information

I.	Crystallographic Structure Refinement Details.....	2
II.	Packing Diagrams Highlighting Noncovalent Interactions.....	7
III.	Powder X-Ray Diffraction Patterns.....	11
IV.	Thermogravimetric Analysis Plots.....	14
V.	Low Temperature Luminescence Measurements.....	17
VI.	Lifetime Measurements.....	19
VII.	Diffuse Reflectance and UV-Vis Absorption Spectroscopy.....	21
VIII.	Supramolecular Interactions.....	26
IX.	Computational Details.....	30
X.	Additional Excitation and Emission Spectra.....	54

I. Crystallographic Structure Refinement Details

All crystallographic details can be found in the refinement section of the corresponding crystallographic information file (CIF). For **1-5**, all non-hydrogen atoms were refined anisotropically after being located in the Fourier difference map. Hydrogens involved with hydrogen bonding (i.e. those present on N or O atoms) were located in the difference map. All O-H distances in carboxylic acids were fixed at 0.84(0.02) Å, O-H distances in water molecules were fixed at 0.88(0.02) Å, and N-H distances were allowed to freely refine. U_{eq} values for H atoms on protonated nitrogens and oxygens were assigned as 1.5 times their carrier atom; remaining H atom U's were assigned as 1.2 times carrier U_{eq} . Thermal ellipsoid plots are shown in Figures S1-S5. For **1**, two lattice waters were disordered over two sites; a constraint was added to the anisotropic displacement parameters of the minor occupant oxygens. Hydrogen atoms could not be found for the minor occupant waters.

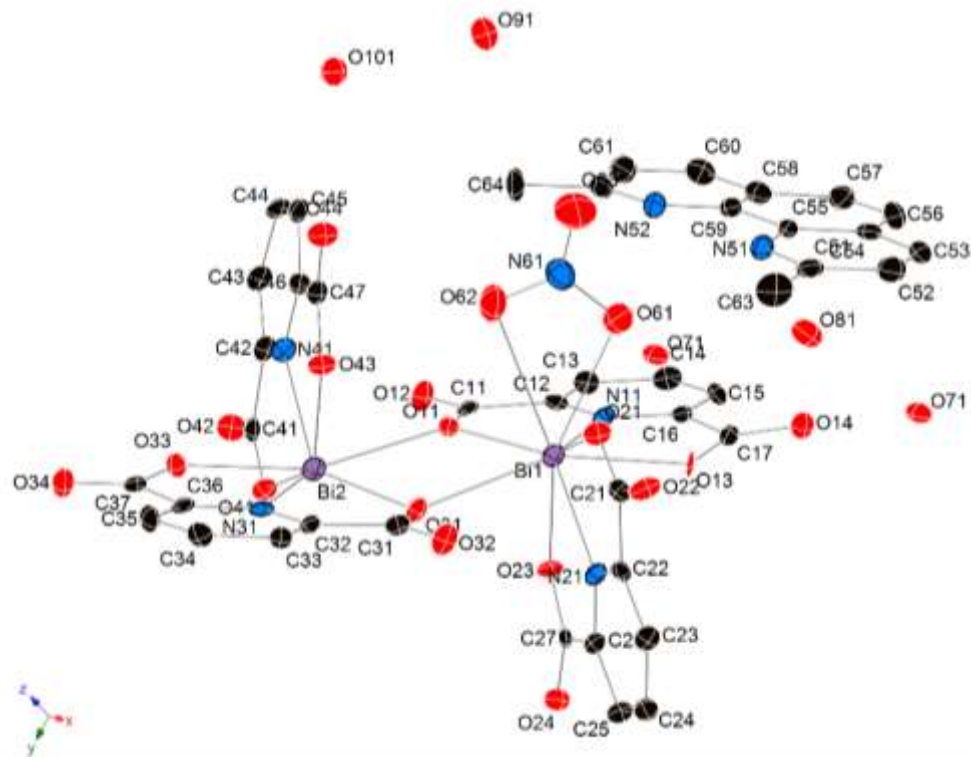


Figure S1. Thermal ellipsoid plot of **1** at 100 K. Ellipsoids are shown at 50% probability. Hydrogen atoms are not shown for clarity. Purple = bismuth; red = oxygen; blue = nitrogen; black = carbon atoms.

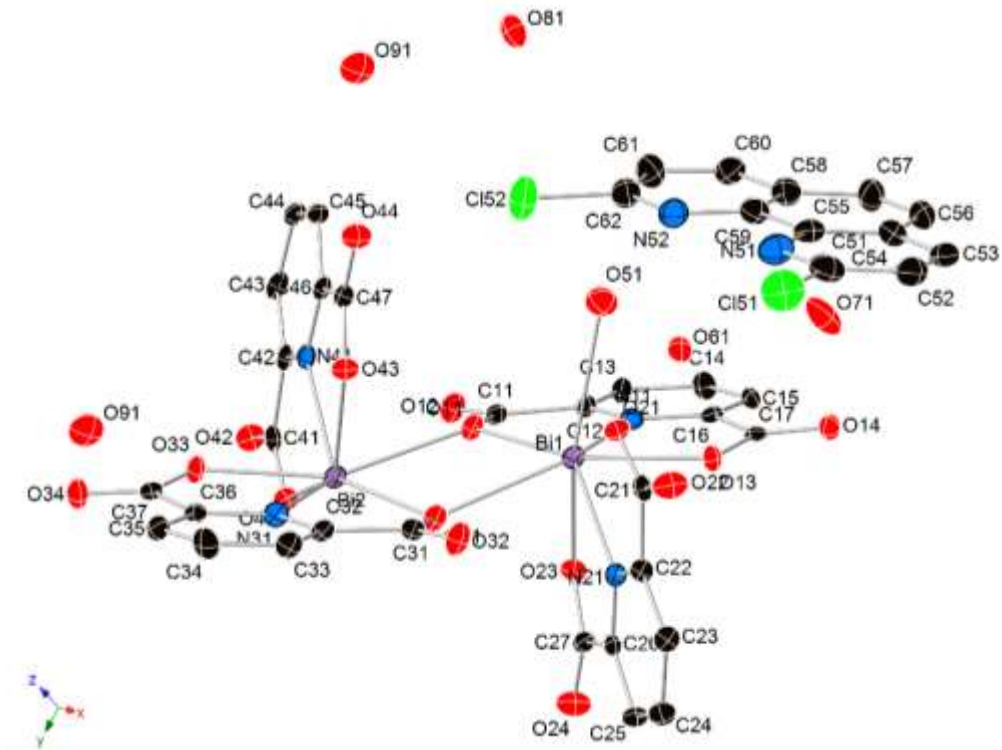


Figure S2. Thermal ellipsoid plot of **2** at 100 K. Ellipsoids are shown at 50% probability. Hydrogen atoms are not shown for clarity. Purple = bismuth; red = oxygen; blue = nitrogen; black = carbon; green = chlorine atoms.

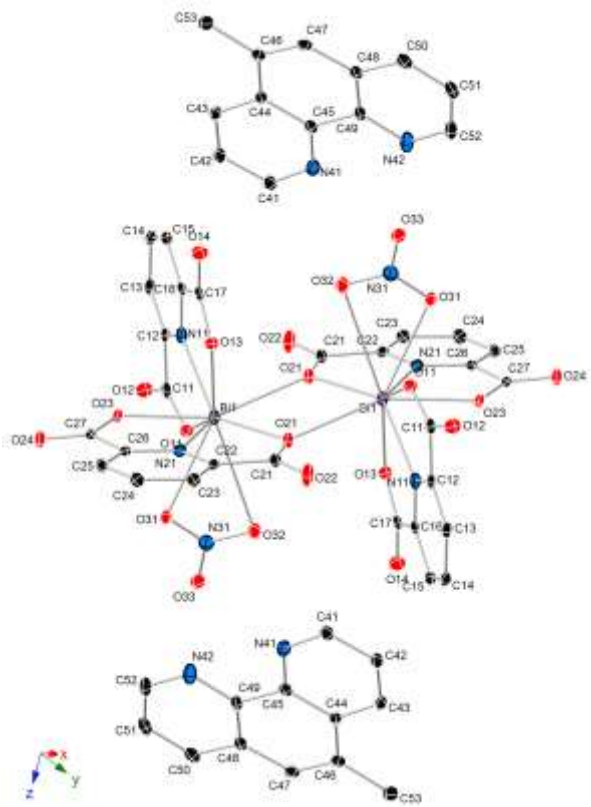


Figure S3. Thermal ellipsoid plot of **3** at 100 K. Ellipsoids are shown at 50% probability. Hydrogen atoms are not shown for clarity. Purple = bismuth; red = oxygen; blue = nitrogen; black = carbon atoms.

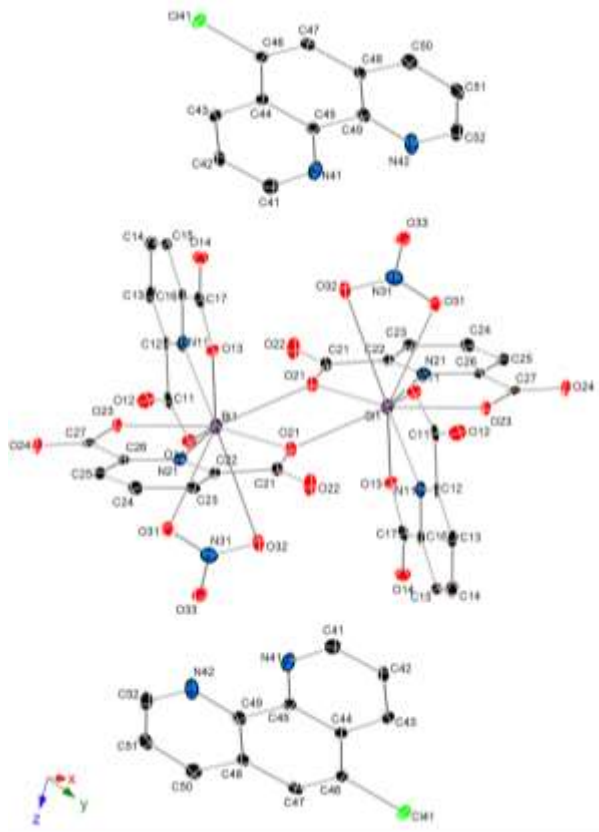


Figure S4. Thermal ellipsoid plot of **4** at 100 K. Ellipsoids are shown at 50% probability. Hydrogen atoms are not shown for clarity. Purple = bismuth; red = oxygen; blue = nitrogen; black = carbon; green = chlorine atoms.

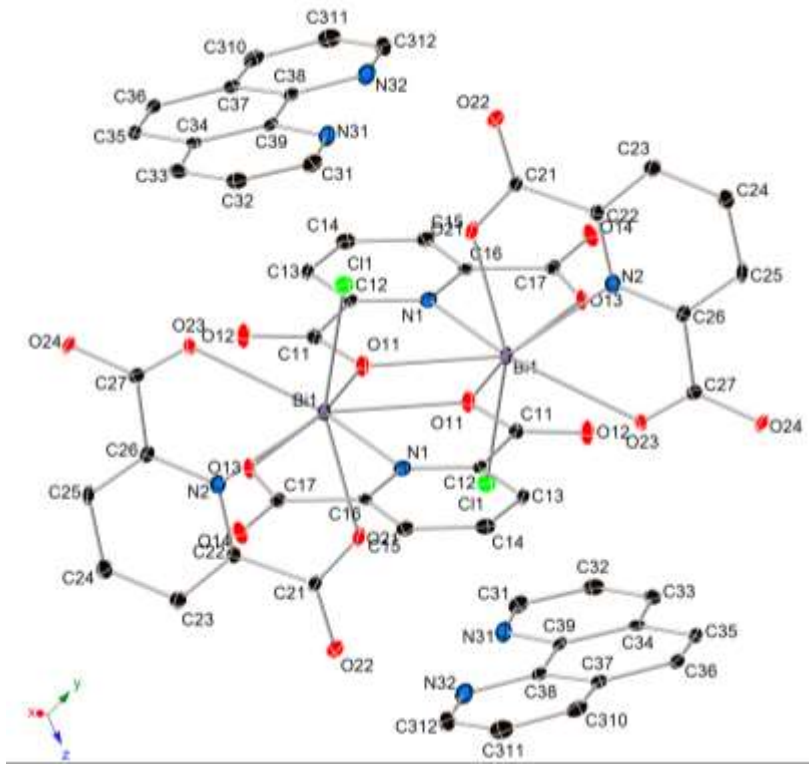


Figure S5. Thermal ellipsoid plot of **5** at 100 K. Ellipsoids are shown at 50% probability. Hydrogen atoms are not shown for clarity. Purple = bismuth; red = oxygen; blue = nitrogen; black = carbon; green = chlorine atoms.

II. Packing Diagrams Highlighting Noncovalent Interactions

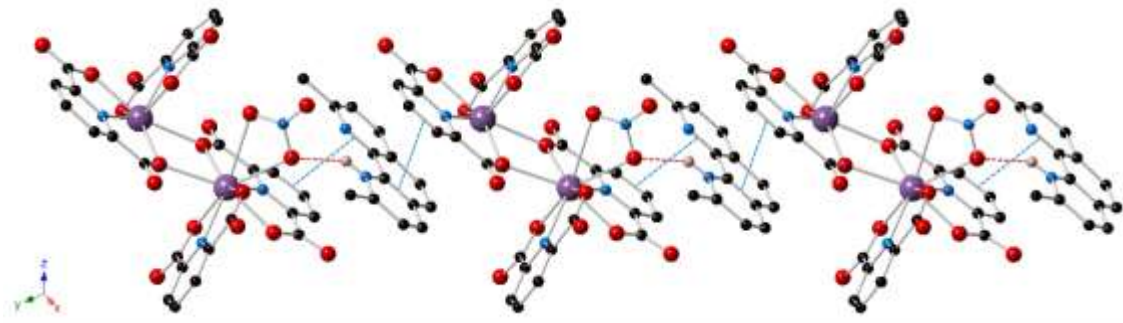


Fig. S6 Packing diagram of **1** depicting the hydrogen bonding between Me₂PhenH and the nitrate anions (red dashed line) and π-π interactions of the PDC···Me₂PhenH···PDC sandwich (blue dashed line). Purple = bismuth; red = oxygen; blue = nitrogen; black = carbon atoms. Hydrogen atoms have been omitted for clarity.

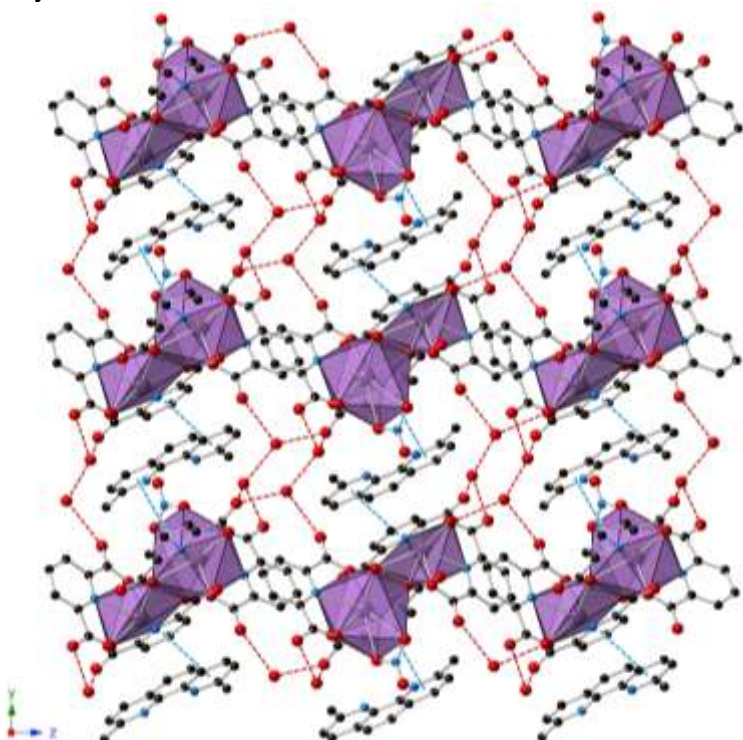


Fig. S7 Packing diagram of **1** depicting the 3-D supramolecular interactions including hydrogen bonding between lattice waters and carboxylates (red dashed line) and π-π interactions of the PDC···Me₂PhenH···PDC sandwich (blue dashed line). Purple = bismuth; red = oxygen; blue = nitrogen; black = carbon atoms. Hydrogen atoms have been omitted for clarity.

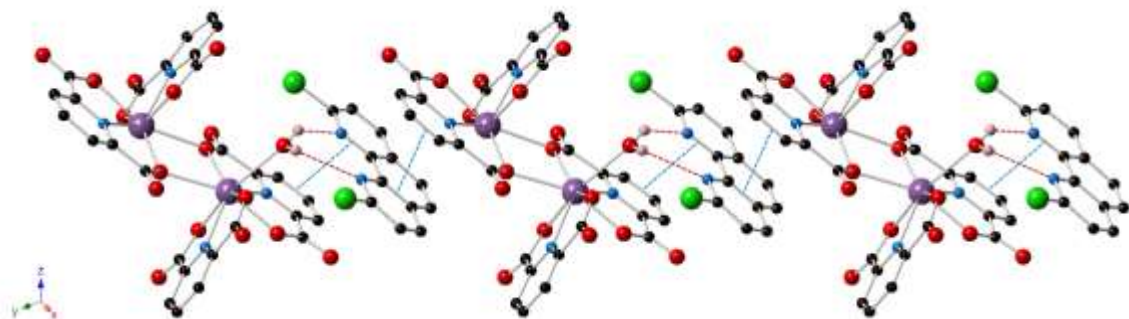


Fig. S8 Packing diagram of **2** depicting the hydrogen bonding between Cl₂Phen and the bound water (red dashed line) and $\pi\text{-}\pi$ interactions of the PDC···Cl₂Phen···PDC sandwich (blue dashed line). Purple = bismuth; red = oxygen; blue = nitrogen; black = carbon; green = chlorine atoms. Hydrogen atoms have been omitted for clarity.

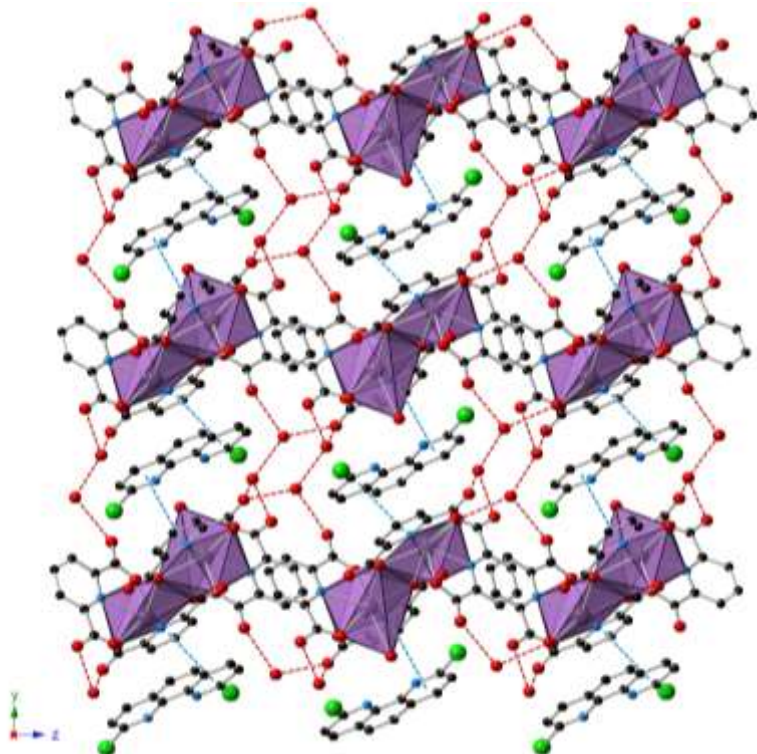


Fig. S9 Packing diagram of **2** depicting the 3-D supramolecular interactions including hydrogen bonding between lattice waters and carboxylates (red dashed line) and $\pi\text{-}\pi$ interactions of the PDC···Cl₂Phen···PDC sandwich (blue dashed line). Purple = bismuth; red = oxygen; blue = nitrogen; black = carbon; green = chlorine atoms. Hydrogen atoms have been omitted for clarity.

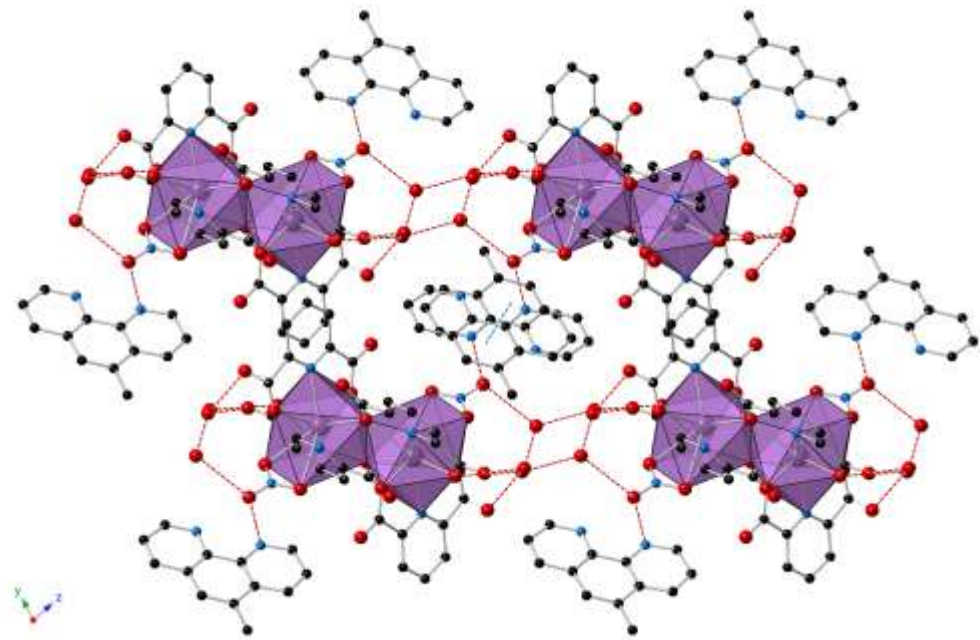


Fig. S10 Packing diagram of **3** depicting the 3-D supramolecular interactions including hydrogen bonding between lattice waters and carboxylates (red dashed line) and $\pi\text{-}\pi$ interactions of the $5\text{-MePhenH}\cdots 5\text{-MePhenH}$ interaction (blue dashed line). Purple = bismuth; red = oxygen; blue = nitrogen; black = carbon atoms. Hydrogen atoms have been omitted for clarity.

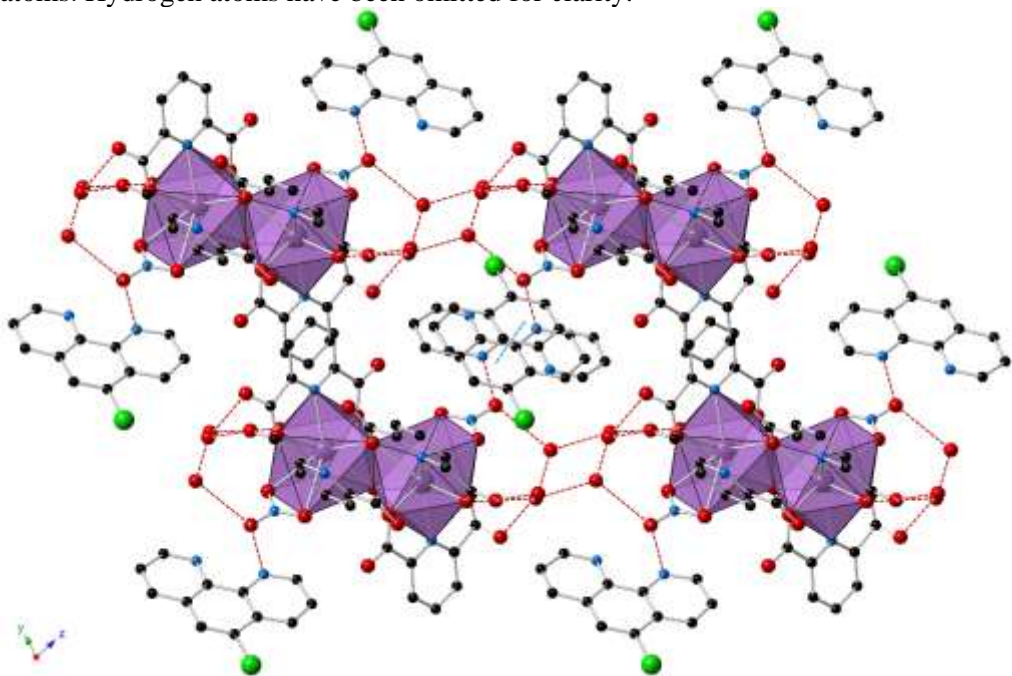


Fig. S11 Packing diagram of **4** depicting the 3-D supramolecular interactions including hydrogen bonding between lattice waters and carboxylates (red dashed line) and $\pi\text{-}\pi$ interactions of the $5\text{-ClPhenH}\cdots 5\text{-ClPhenH}$ interaction (blue dashed line). Purple = bismuth; red = oxygen; blue = nitrogen; black = carbon; green = chlorine atoms. Hydrogen atoms have been omitted for clarity.

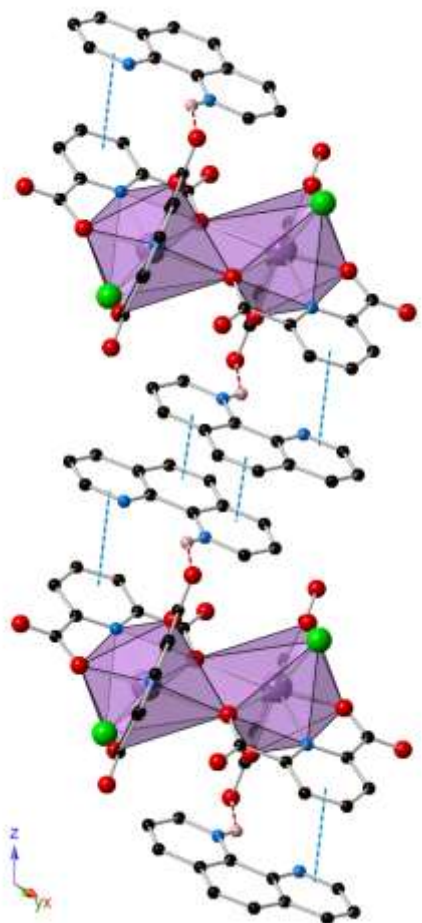


Fig. S12 Packing diagram of **5** depicting the PDC···PhenH···PhenH···PDC π - π interactions (blue dashed line) and hydrogen bonding (red dashed lines). Purple = bismuth; red = oxygen; blue = nitrogen; black = carbon; green = chlorine atoms. Hydrogen atoms other than those bonded to nitrogens have been omitted for clarity.

III. Powder X-ray Diffraction Patterns

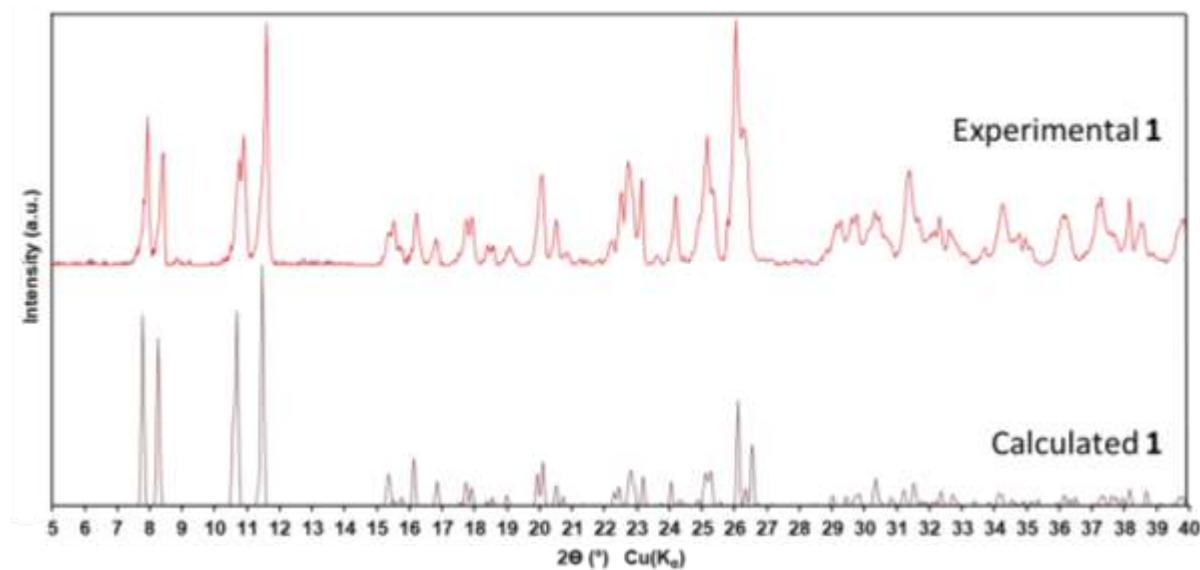


Figure S13. Experimental Powder X-ray Diffraction pattern for **1** (red) overlaid with the pattern calculated from the single crystal data collected at 100 K (black).

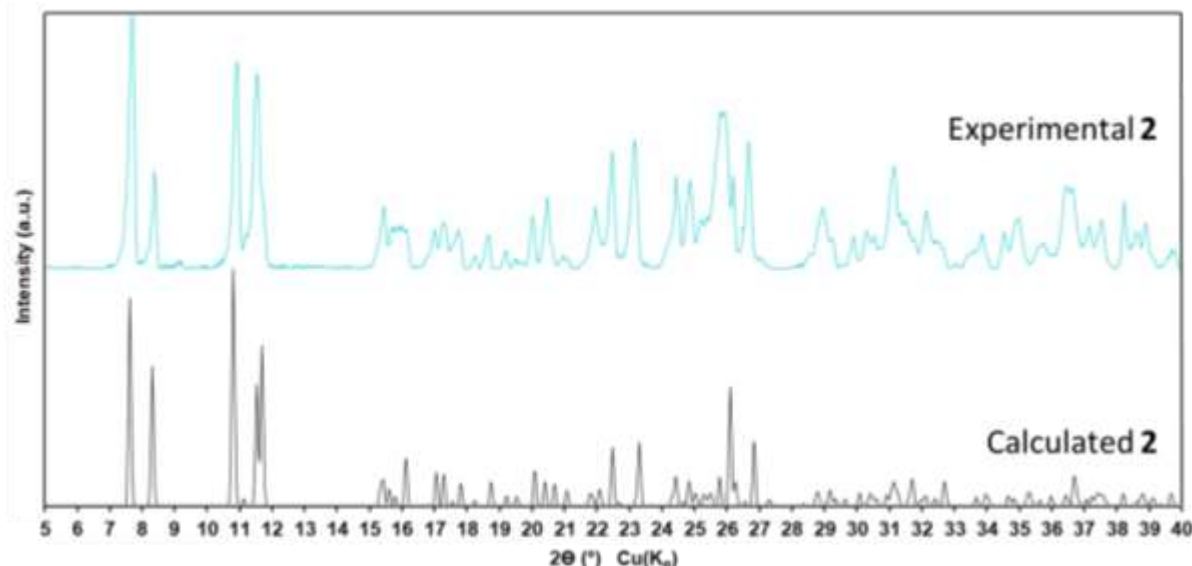


Figure S14. Experimental Powder X-ray Diffraction pattern for **2** (blue) overlaid with the pattern calculated from the single crystal data collected at 100 K (black).

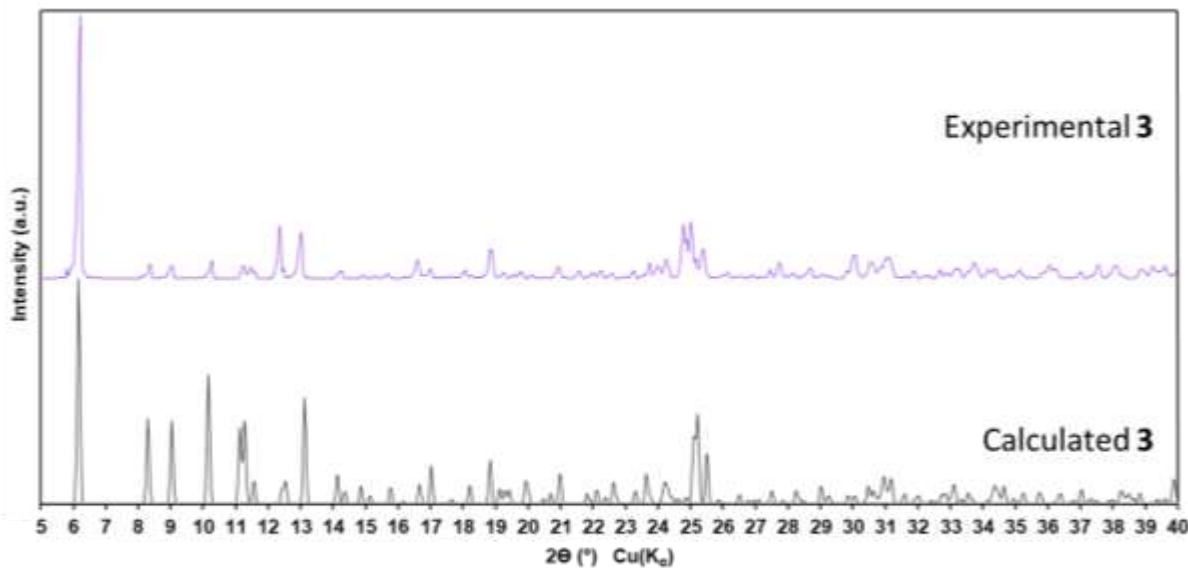


Figure S15. Experimental Powder X-ray Diffraction pattern for **3** (violet) overlaid with the pattern calculated from the single crystal data collected at 100 K (black).

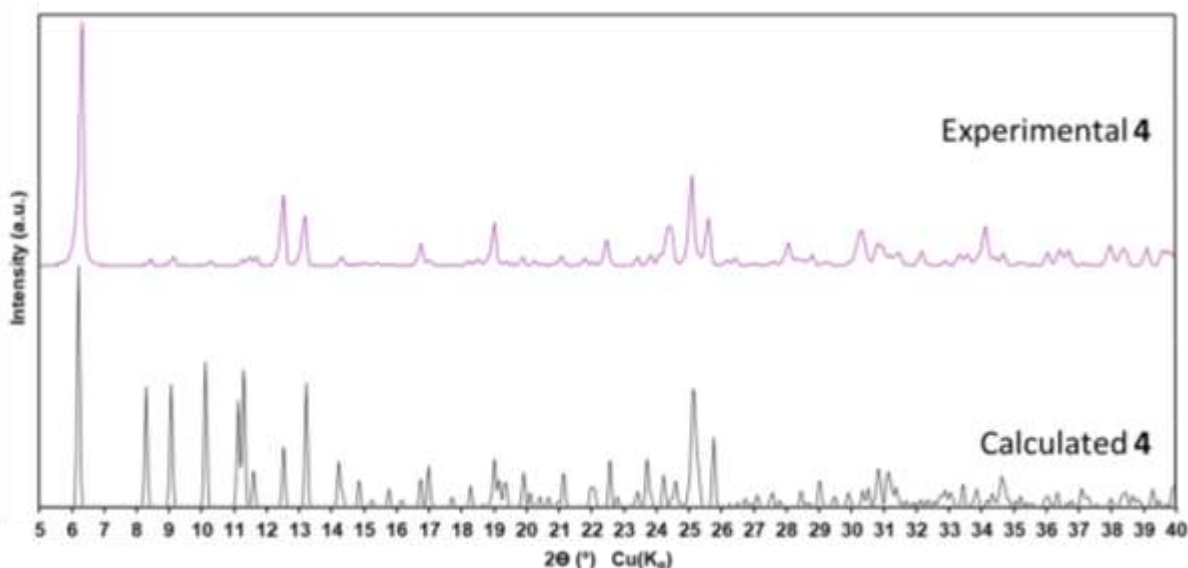


Figure S16. Experimental Powder X-ray Diffraction pattern for **4** (purple) overlaid with the pattern calculated from the single crystal data collected at 100 K (black).

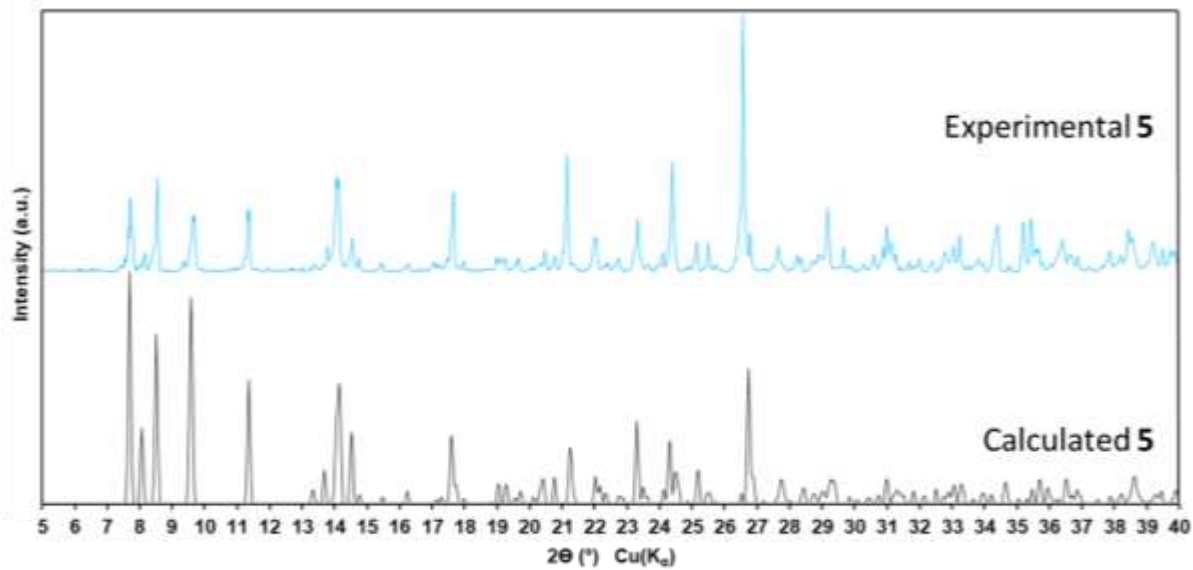


Figure S17. Experimental Powder X-ray Diffraction pattern for **5** (blue) overlaid with the pattern calculated from the single crystal data collected at 100 K (black).

IV. Thermogravimetric Analysis Plots

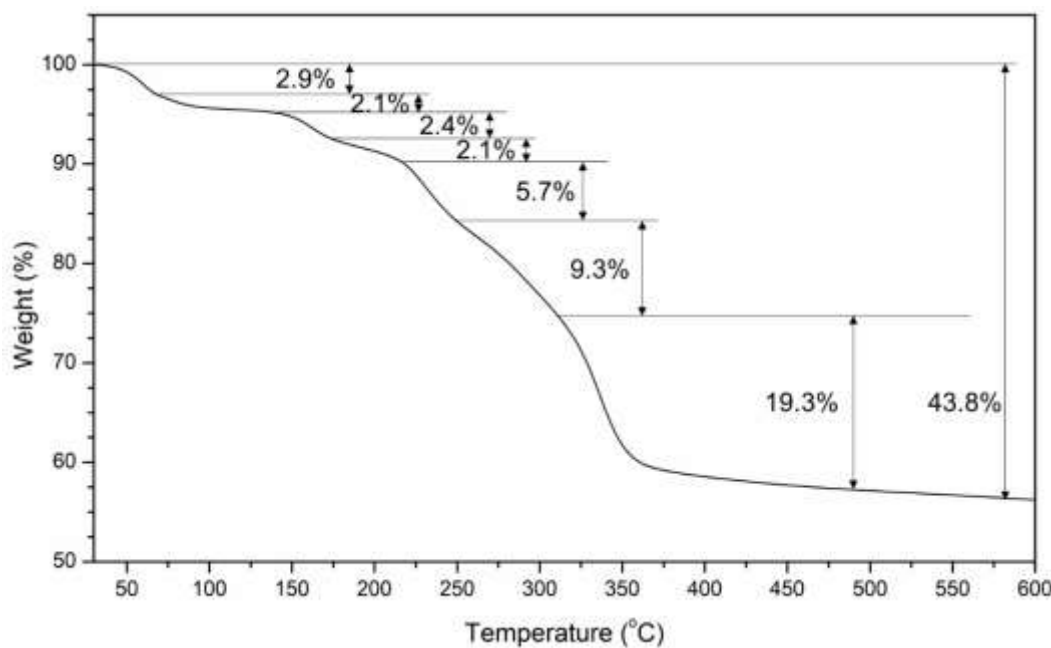


Figure S18. Thermogravimetric analysis of **1** collected from 30-600 °C at a rate of 5 °C per minute, with annotations.

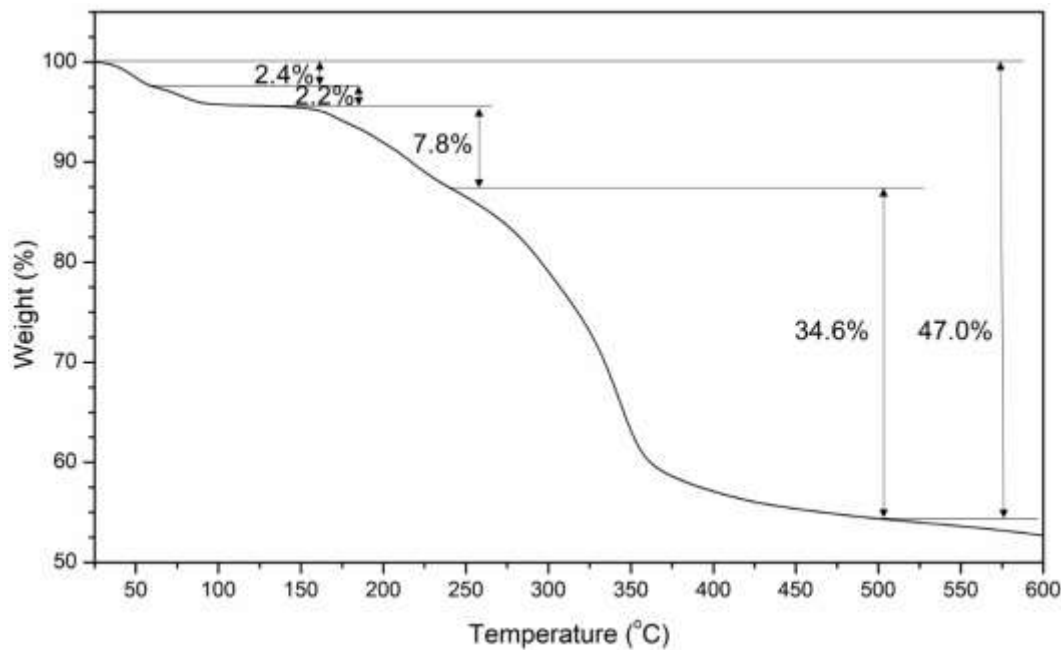


Figure S19. Thermogravimetric analysis of **2** collected from 25-600 °C at a rate of 5 °C per minute, with annotations.

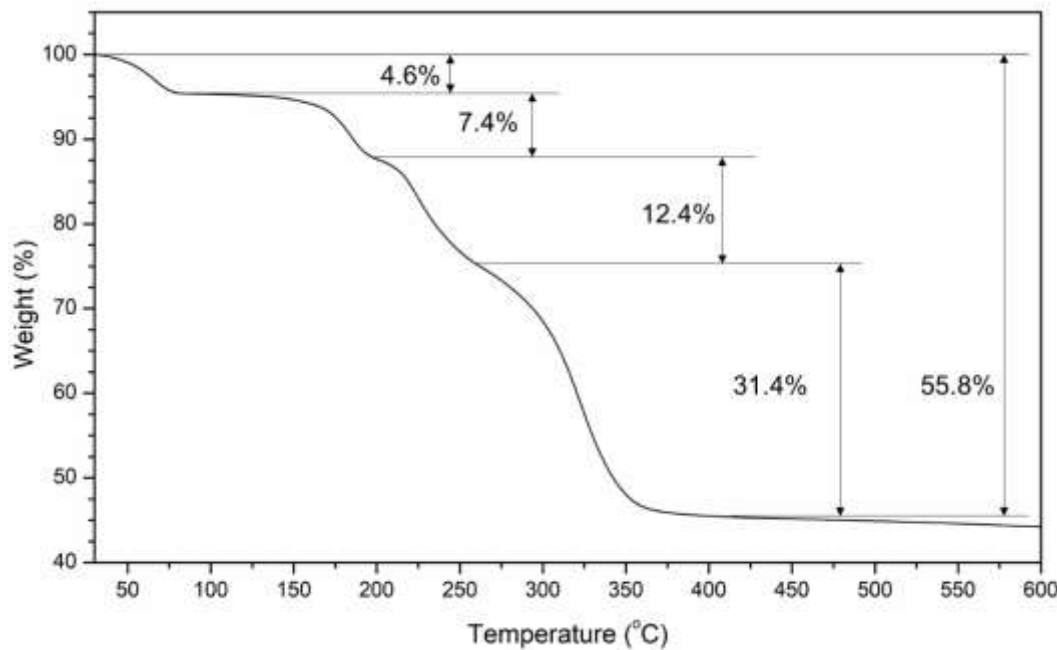


Figure S20. Thermogravimetric analysis of **3** collected from 30-600 °C at a rate of 5 °C per minute, with annotations.

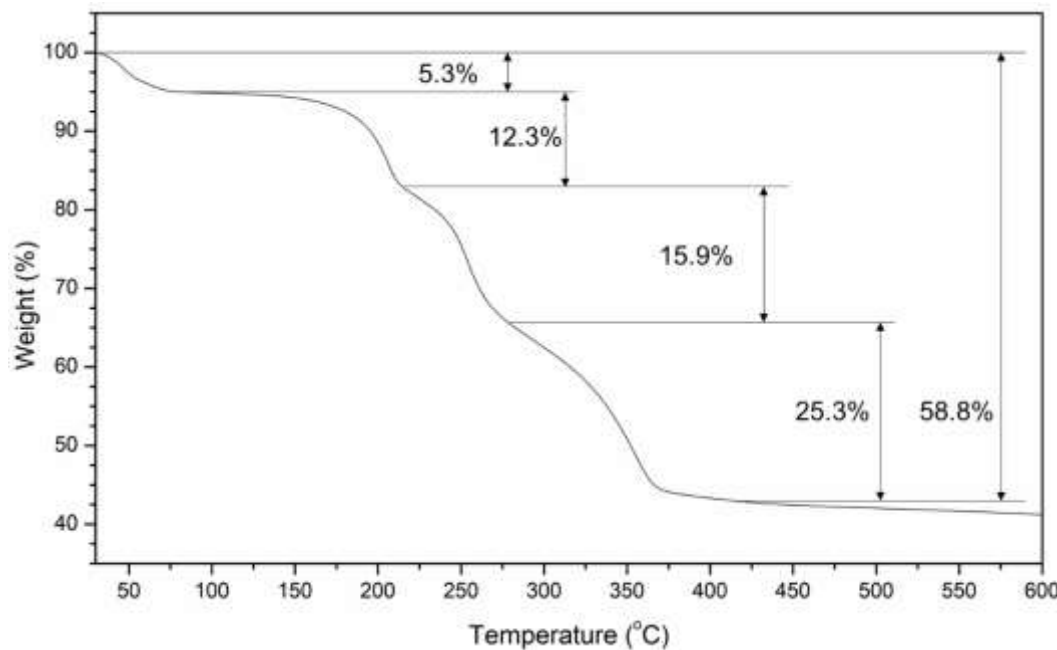


Figure S21. Thermogravimetric analysis of **4** collected from 30-600 °C at a rate of 5 °C per minute, with annotations.

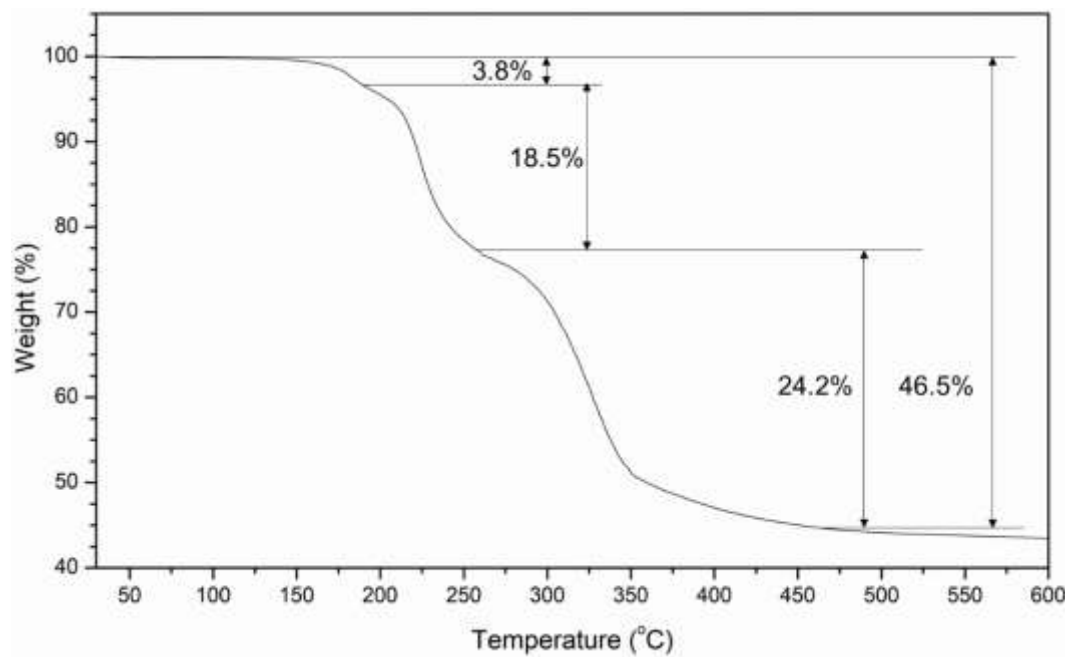


Figure S22. Thermogravimetric analysis of **5** collected from 30-600 °C at a rate of 5 °C per minute, with annotations.

V. Low Temperature Luminescence Measurements

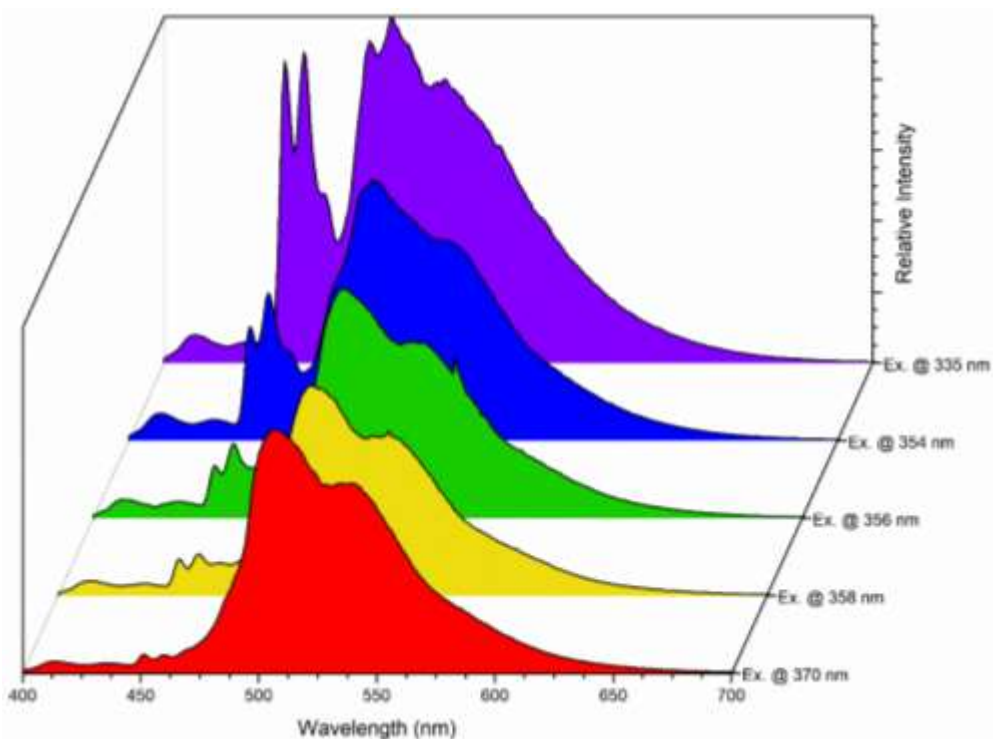


Figure S23. Emission spectra of compound **2** at 77 K displaying excitation dependent color tuning. Higher energy emission peaks grow in as excitation wavelength decreases.

CIE 1931

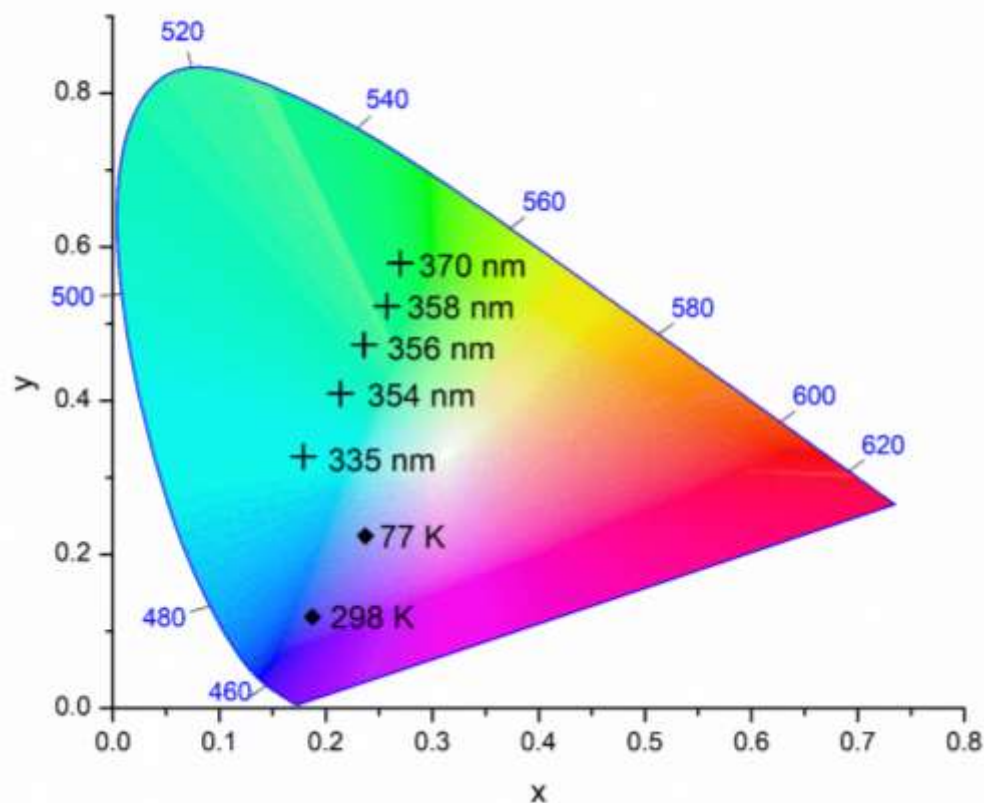


Figure S24. CIE 1931 Chromaticity diagram showing the color shift of **2** (+ signs) at 77 K upon changing the excitation wavelength, and the color shift of **4** (diamonds) upon cooling from RT to 77 K.

VI. Lifetime Measurements

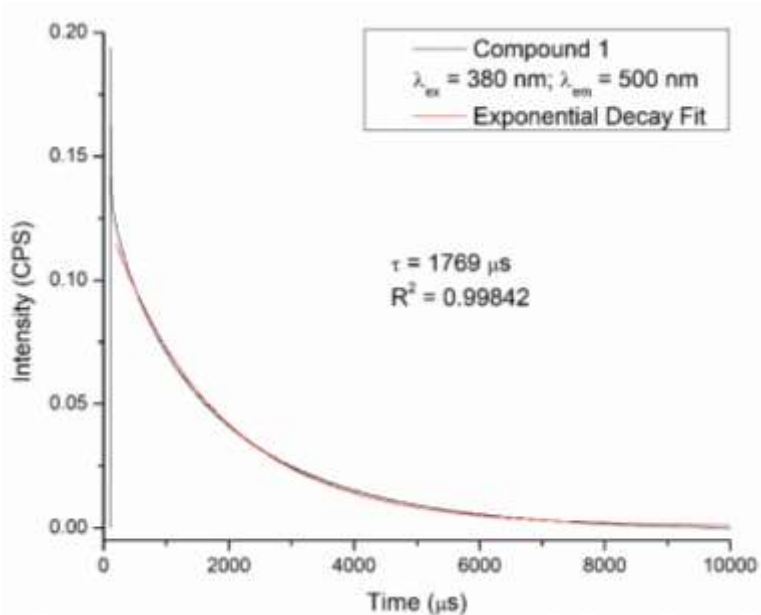


Figure S25. Phosphorescence decay plot for compound 1 fit with a single exponential decay function. Excitation at 380 nm; emission at 500 nm.

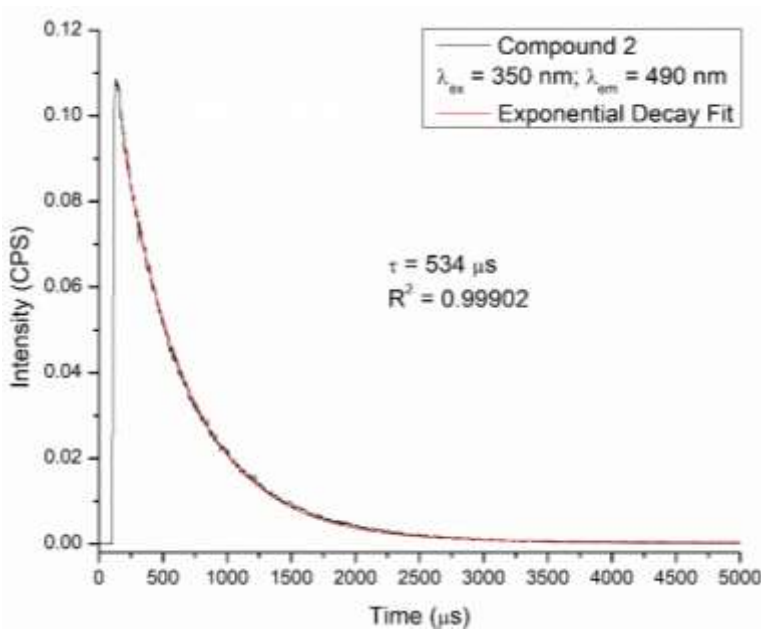


Figure S26. Phosphorescence decay plot for compound 2 fit with a single exponential decay function. Excitation at 350 nm; emission at 490 nm.

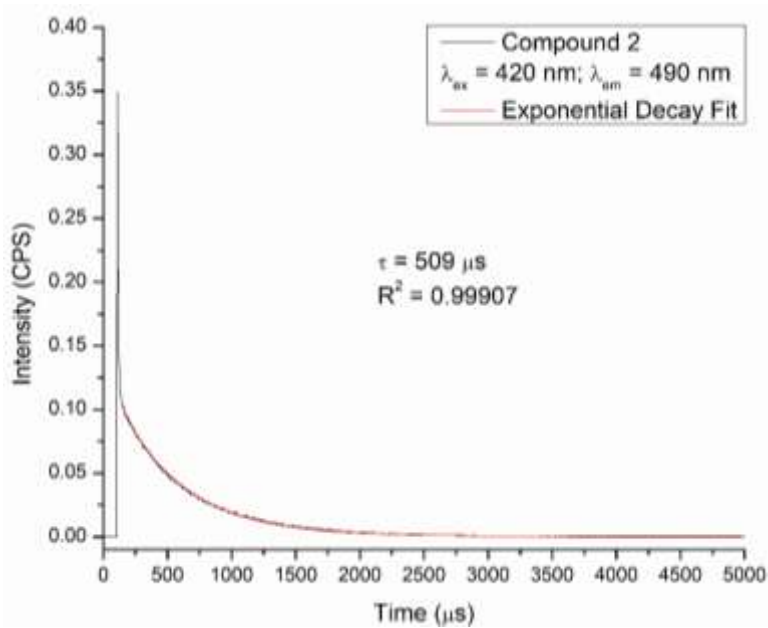


Figure S27. Phosphorescence decay plot for compound **2** fit with a single exponential decay function. Excitation at 420 nm; emission at 490 nm.

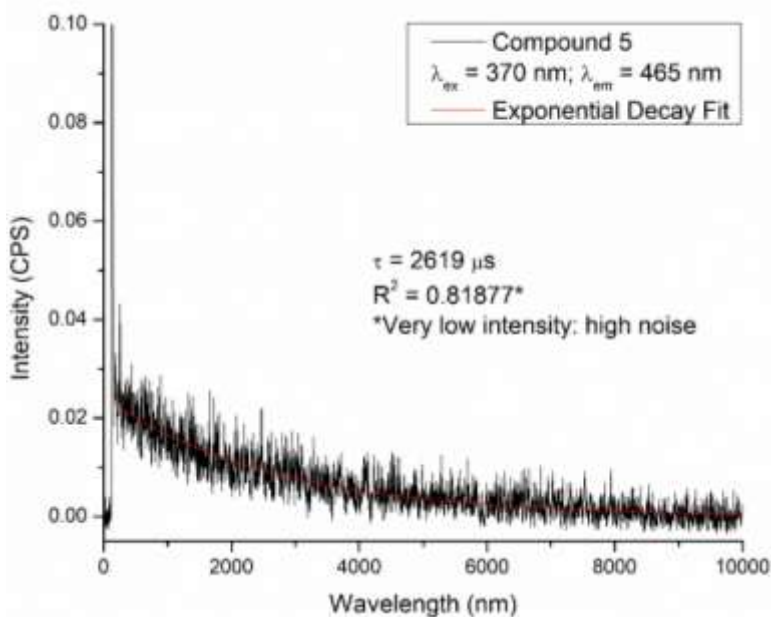


Figure S28. Phosphorescence decay plot for compound **5** fit with a single exponential decay function. Excitation at 370 nm; emission at 465 nm. Note the low signal-to-noise ratio that gives rise to the poor R^2 value.

VII. Diffuse Reflectance and UV-Vis Absorbance Spectroscopy

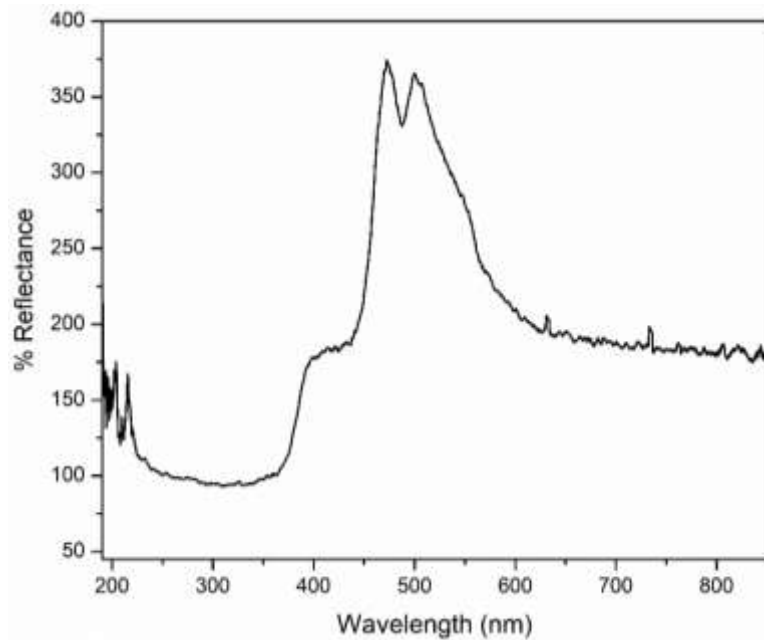


Figure S29. Diffuse reflectance data for compound **1**.

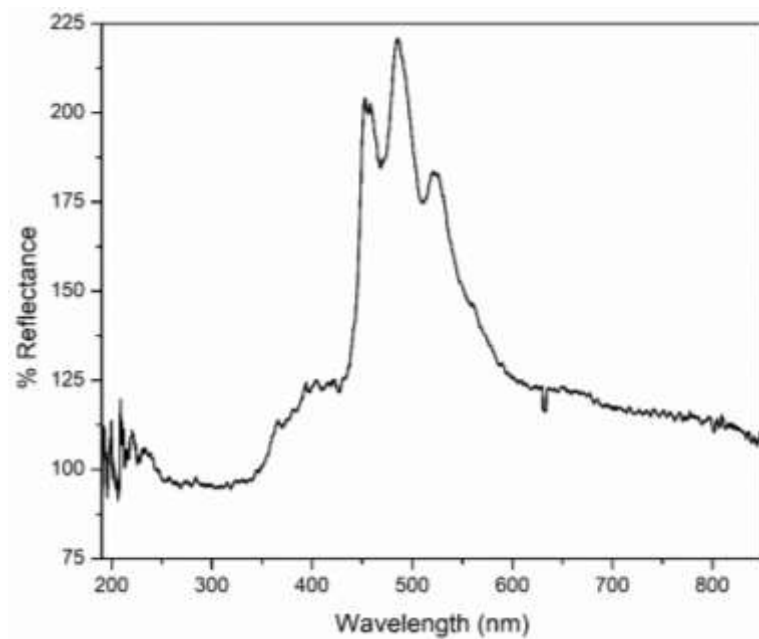


Figure S30. Diffuse reflectance data for compound **2**.

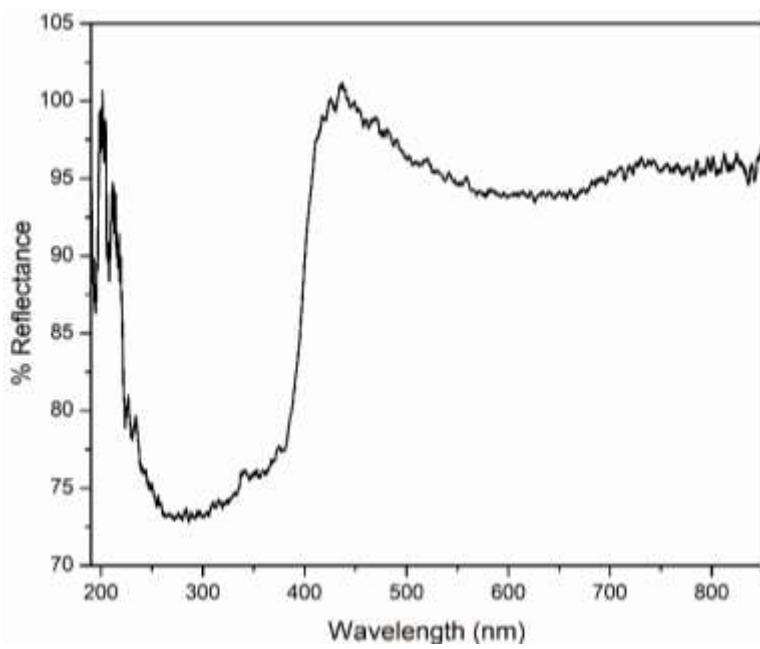


Figure S31. Diffuse reflectance data for compound **3**.

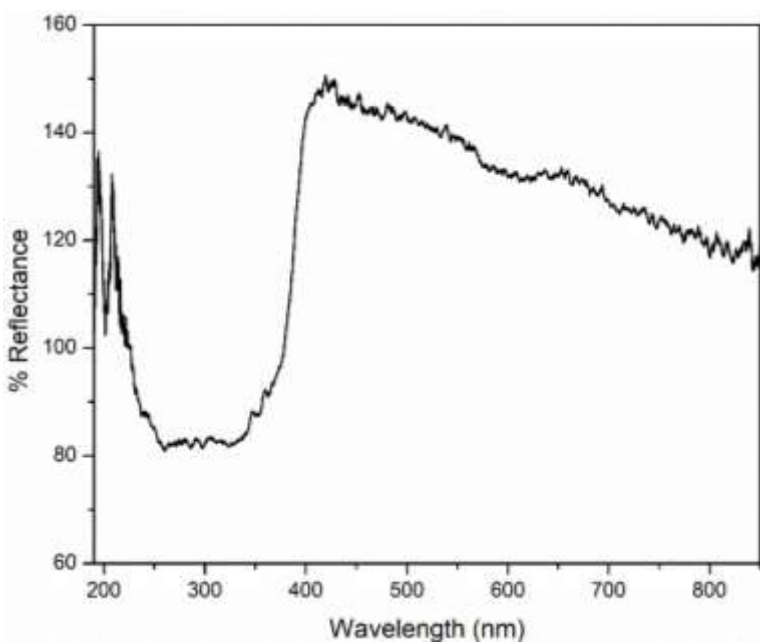


Figure S32. Diffuse reflectance data for compound **4**.

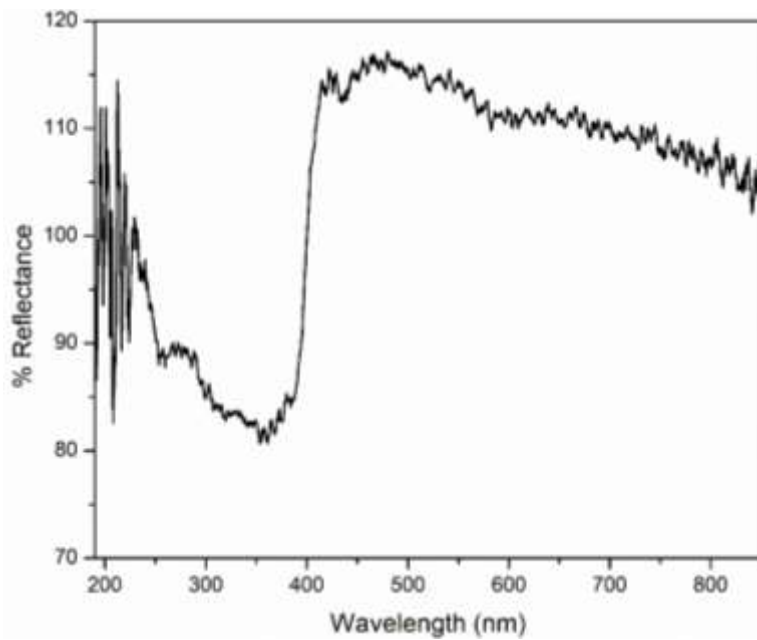


Figure S33. Diffuse reflectance data for compound **5**.

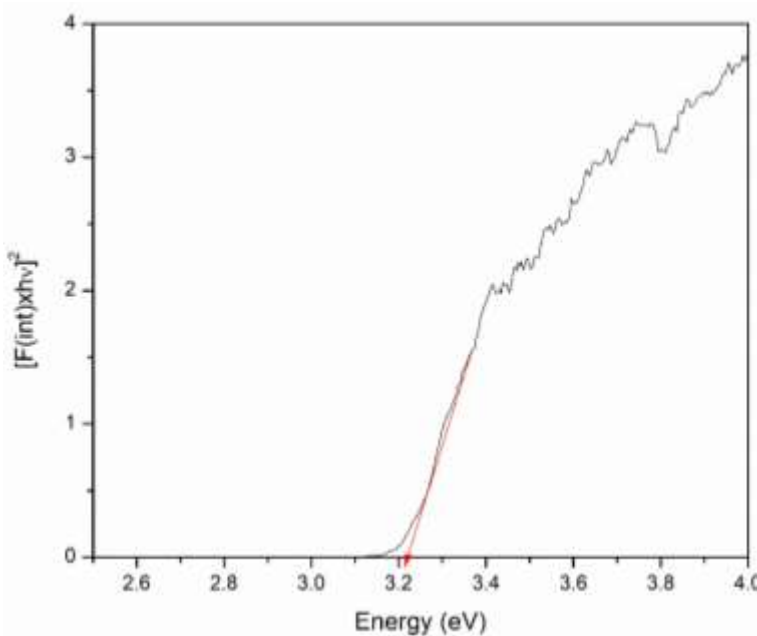


Figure S34. Tauc plot for compound **1** calculated from normalized diffuse reflectance data using the Kubelka-Munk equation.

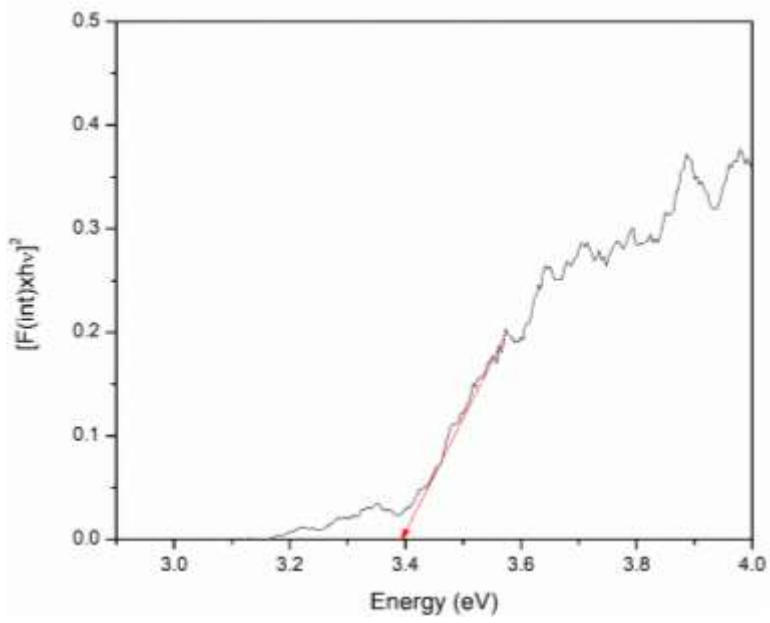


Figure S35. Tauc plot for compound 2 calculated from normalized diffuse reflectance data using the Kubelka-Munk equation.

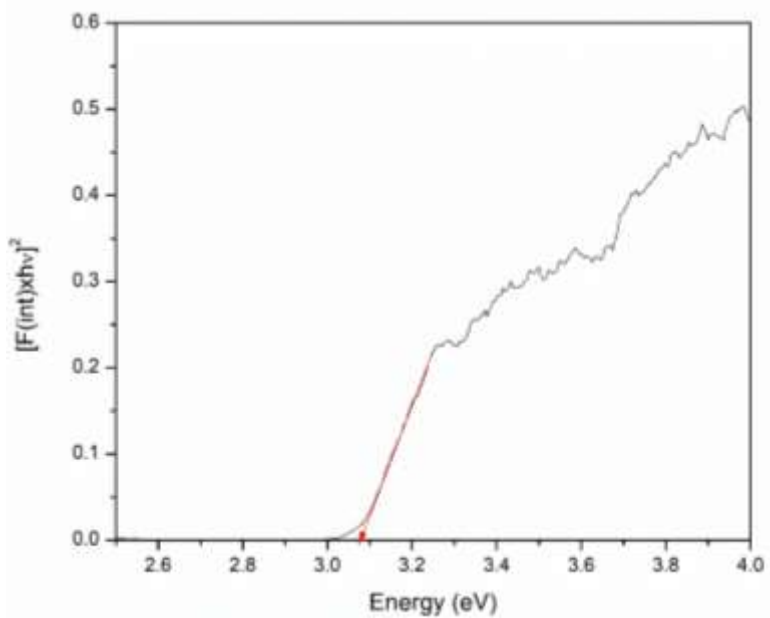


Figure S36. Tauc plot for compound 3 calculated from normalized diffuse reflectance data using the Kubelka-Munk equation.

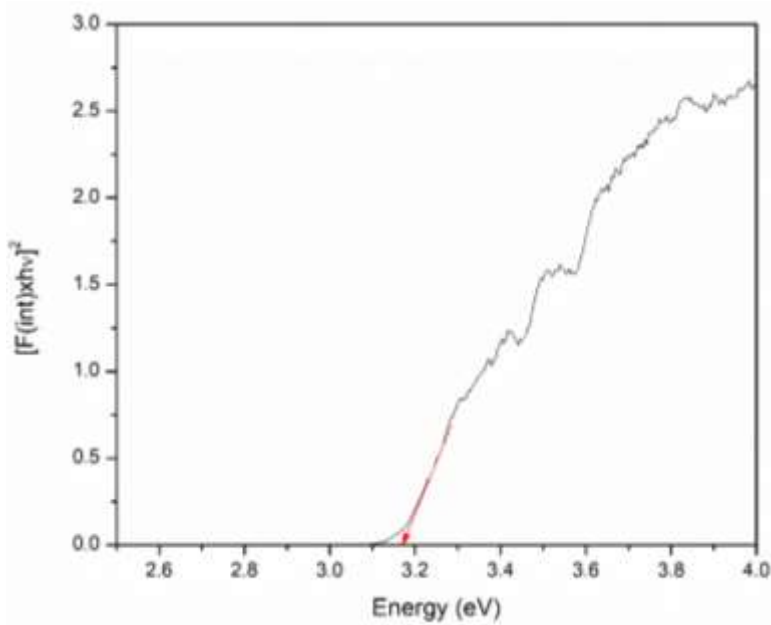


Figure S37. Tauc plot for compound **4** calculated from normalized diffuse reflectance data using the Kubelka-Munk equation.

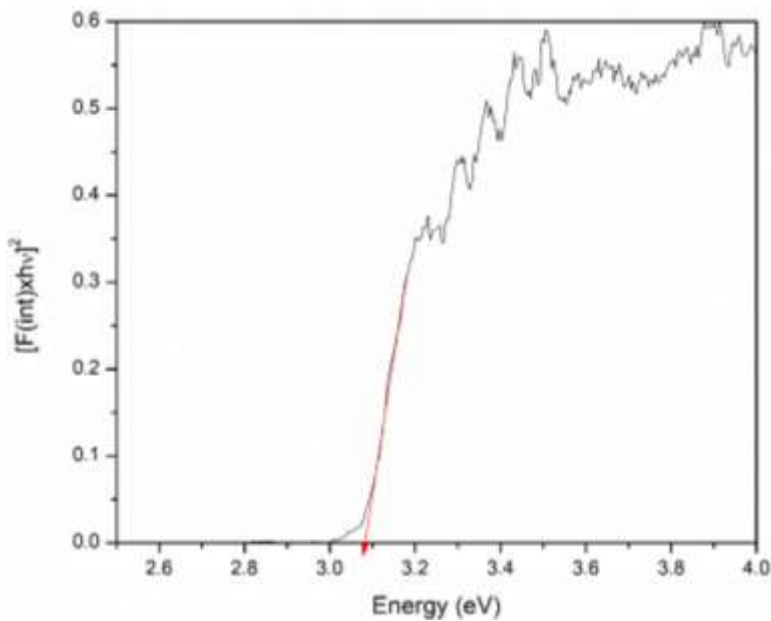


Figure S38. Tauc plot for compound **5** calculated from normalized diffuse reflectance data using the Kubelka-Munk equation.

VIII. Supramolecular Interactions

Noncovalent interactions including π - π stacking, metal- π interactions, and hydrogen bonding were calculated using the PLATON software suite *via* the “Calc All” feature. The supramolecular interactions are summarized in Tables S1-S5.

Table S1. Supramolecular interactions for **1**. C_{g1} is the centroid formed by N11, C12, C13, C14, C15, C16. C_{g3} is the centroid formed by N31, C32, C33, C34, C35, C36. C_{g5} is the centroid formed by N51, C51, C52, C53, C54, C55. C_{g6} is the centroid formed by N52, C58, C59, C60, C61, C62. C_{g7} is the centroid formed by C54, C55, C56, C57, C58, C59.

Interaction	Distance (\AA), $C_g\cdots C_g$ or $M\cdots C_g$	β ($^\circ$)	Distance (\AA), $D\cdots H\cdots A$	Angle ($^\circ$), $D\cdots H\cdots A$
$C_{g1}\cdots C_{g6}$	3.612(4)	17.6	-	-
$C_{g3}\cdots C_{g5}$	3.690(4)	22.9	-	-
$\text{Bi}(2)\cdots C_{g7}$	3.636	12.98	-	-
O(22)-H---O(71)	-	-	2.462(7)	171(5)
O(42)-H---O(91)	-	-	2.436(8)	172(10)
N(51)-H---O(61)	-	-	2.738(8)	144(8)
N(51)-H---N(52) <i>Intra</i>	-	-	2.709(9)	103(7)
O(71)-H---O(81)	-	-	2.606(8)	171(5)
O(71)-H---O(14)	-	-	2.693(8)	156(7)
O(81)-H---O(14)	-	-	2.812(8)	161(9)
O(81)-H---O(24)	-	-	2.797(7)	166(8)
O(91)-H---O(101)	-	-	2.627(9)	151(8)
O(91)-H---O(34)	-	-	2.726(9)	148(6)
O(101)-H---O(33)	-	-	2.877(8)	157(9)
O(101)-H---O(44)	-	-	2.758(8)	163(10)

Table S2. Supramolecular interactions for **2**. C_{g1} is the centroid formed by N11, C12, C13, C14, C15, C16. C_{g3} is the centroid formed by N31, C32, C33, C34, C35, C36. C_{g5} is the centroid formed by N51, C51, C52, C53, C54, C55. C_{g6} is the centroid formed by N52, C58, C59, C60, C61, C62. C_{g7} is the centroid formed by C54, C55, C56, C57, C58, C59.

Interaction	Distance (Å), C_g --- C_g or M--- C_g	β (°)	Distance (Å), D-H---A	Angle (°), D-H---A
C_{g1} --- C_{g6}	3.562(3)	13.0	-	-
C_{g3} --- C_{g5}	3.600(3)	16.7	-	-
Bi(2)--- C_{g7}	3.714	19.36	-	-
O(22)-H---O(61)	-	-	2.450(5)	171(3)
O(42)-H---O(81)	-	-	2.487(5)	172(3)
O(51)-H---N(52)	-	-	2.924(7)	137(5)
O(61)-H---O(71)	-	-	2.579(6)	179(6)
O(61)-H---O(14)	-	-	2.665(5)	164(5)
O(71)-H---O(14)	-	-	2.794(5)	160(8)
O(71)-H---O(24)	-	-	2.782(6)	157(6)
O(81)-H---O(91)	-	-	2.671(6)	168(5)
O(81)-H---O(34)	-	-	2.721(5)	153(5)
O(91)-H---O(33)	-	-	2.934(5)	163(6)
O(91)-H---O(44)	-	-	2.800(5)	168(4)

Table S3. Hydrogen bonding interactions for **3**. No π - π interactions with C_g --- C_g distance $< 4.0 \text{ \AA}$.

Interaction	Distance (\AA), D-H---A	Angle ($^\circ$), D-H---A
O(12)-H---O(51)	2.517(3)	172(2)
N(41)-H---O(33)	2.795(3)	159
O(51)-H---O(61)	2.682(3)	171(3)
O(51)-H---O(24)	2.747(3)	147(2)
O(61)-H---O(71)	2.755(3)	166(4)
O(61)-H---O(33)	2.794(3)	163(3)
O(71)-H---O(61)	2.863(3)	157(3)
O(71)-H---O(23)	2.988(3)	173(3)

Table S4. Hydrogen bonding interactions for **4**. No π - π interactions with C_g --- C_g distance $< 4.0 \text{ \AA}$.

Interaction	Distance (\AA), D-H---A	Angle ($^\circ$), D-H---A
O(12)-H---O(51)	2.494(3)	170(3)
N(41)-H---O(33)	2.780(4)	163(3)
O(51)-H---O(61)	2.672(4)	165(3)
O(51)-H---O(24)	2.745(3)	141(4)
O(61)-H---O(71)	2.757(4)	165(4)
O(61)-H---O(33)	2.806(3)	165(4)
O(71)-H---O(61)	2.863(4)	168(4)
O(71)-H---O(23)	2.965(3)	167(3)

Table S5. Supramolecular interactions for **5**. C_{g2} is the centroid formed by N21, C22, C23, C24, C25, C26. C_{g3} is the centroid formed by N31, C31, C32, C33, C34, C35. C_{g4} is the centroid formed by N32, C38, C39, C40, C41, C42. C_{g5} is the centroid formed by C34, C35, C36, C37, C38, C39.

Interaction	Distance (Å), C_g -- C_g	β (°)	Distance (Å), D-H---A	Angle (°), D-H---A
C_{g2} -- C_{g4}	3.771(1)	21.4	-	-
C_{g3} -- C_{g4}	3.701(1)	25.2		
C_{g3} -- C_{g5}	3.573(1)	18.4	-	-
O(12)-H---O(41)	-	-	2.476(2)	179(3)
N(31)-H---O(13)	-	-	2.988(2)	119(3)
N(31)-H---O(14)	-	-	3.129(3)	133(3)
O(41)-H---O(51)	-	-	2.665(3)	173(2)
O(41)-H---O(61)	-	-	2.628(3)	176(3)
O(51)-H---Cl(1)	-	-	3.293(2)	149(3)
O(51)-H---O(71)	-	-	2.757(3)	163(5)
O(61)-H---Cl(1)	-	-	3.249(2)	176(3)
O(61)-H---O(22)	-	-	2.752(3)	174(3)
O(71)-H---O(14)	-	-	2.825(3)	174(3)
O(71)-H---O(23)	-	-	2.839(2)	175(2)

IX. Computational Details

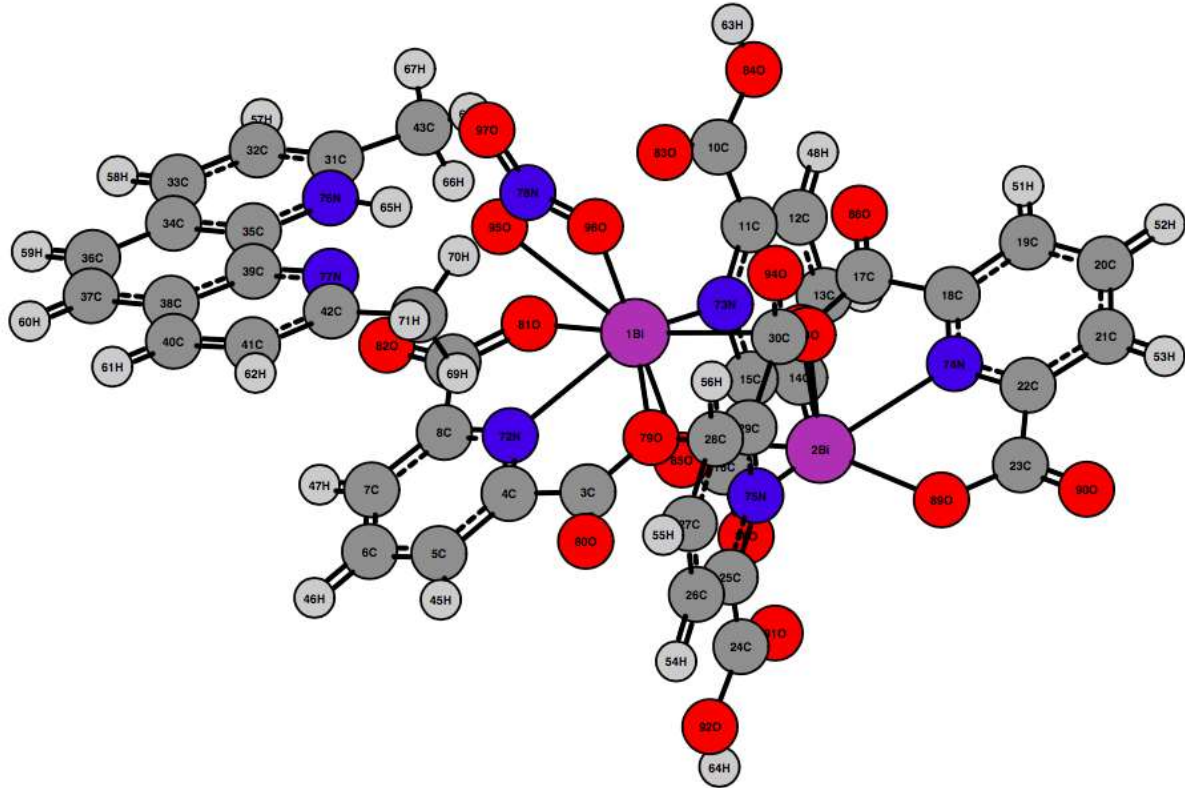


Figure S39. DFT calculated ground state structures for **1**.

Table S6. DFT calculated ground state parameters for **1**.

Bond	Length (Å)	Bond	Length (Å)	Bond	Length (Å)
Bi1 - N72	2.4481	C25 - N75	1.3360	C7 - C6	1.3922
Bi1 - N73	2.5868	C26 - C25	1.3891	C8 - C7	1.3917
Bi1 - O79	2.5345	C27 - C26	1.3962	C8 - N72	1.3329
Bi1 - O81	2.3447	C28 - C27	1.3879	C9 - C8	1.5246
Bi1 - O83	2.9021	C29 - C28	1.3973	C9 - O81	1.2867
Bi1 - O85	2.2566	C29 - N75	1.3264	C9 - O82	1.2278
Bi1 - O87	2.6525	C3 - O79	1.2911	N78 - O95	1.3033
Bi1 - O95	2.6994	C3 - O80	1.2274	N78 - O96	1.2426
Bi1 - O96	2.9583	C30 - C29	1.5216	N78 - O97	1.2254
Bi2 - N74	2.4410	C30 - O93	1.3100	C21 - C20	1.3925
Bi2 - N75	2.5261	C30 - O94	1.2112	C22 - C21	1.3917
Bi2 - O79	2.6423	C31 - N76	1.3384	C22 - N74	1.3339
Bi2 - O87	2.5057	C32 - C31	1.4075	C23 - C22	1.5266
Bi2 - O89	2.2829	C33 - C32	1.3722	C23 - O89	1.3009
Bi2 - O91	2.8796	C34 - C33	1.4136	C23 - O90	1.2156
Bi2 - O93	2.1785	C35 - C34	1.4096	C24 - O91	1.2089
C10 - O83	1.2109	C35 - N76	1.3651	C24 - O92	1.3395
C10 - O84	1.3406	C36 - C34	1.4306	C25 - C24	1.4950
C11 - C10	1.4942	C37 - C36	1.3594	C18 - N74	1.3342
C11 - N73	1.3355	C38 - C37	1.4294	C19 - C18	1.3909
C12 - C11	1.3901	C39 - C35	1.4423	C20 - C19	1.3936
C13 - C12	1.3960	C39 - C38	1.4187	C44 - H71	1.0914
C14 - C13	1.3875	C39 - N77	1.3458	C5 - C4	1.3918
C15 - C14	1.3976	C4 - C3	1.5216	C6 - C5	1.3918
C15 - N73	1.3282	C4 - N72	1.3333		
C16 - C15	1.5266	C40 - C38	1.4124		
C16 - O85	1.2977	C41 - C40	1.3732		
C16 - O86	1.2178	C42 - C41	1.4204		
C17 - O87	1.2956	C42 - N77	1.3248		
C17 - O88	1.2245	C43 - C31	1.4914		
C18 - C17	1.5222	C44 - C42	1.5031		

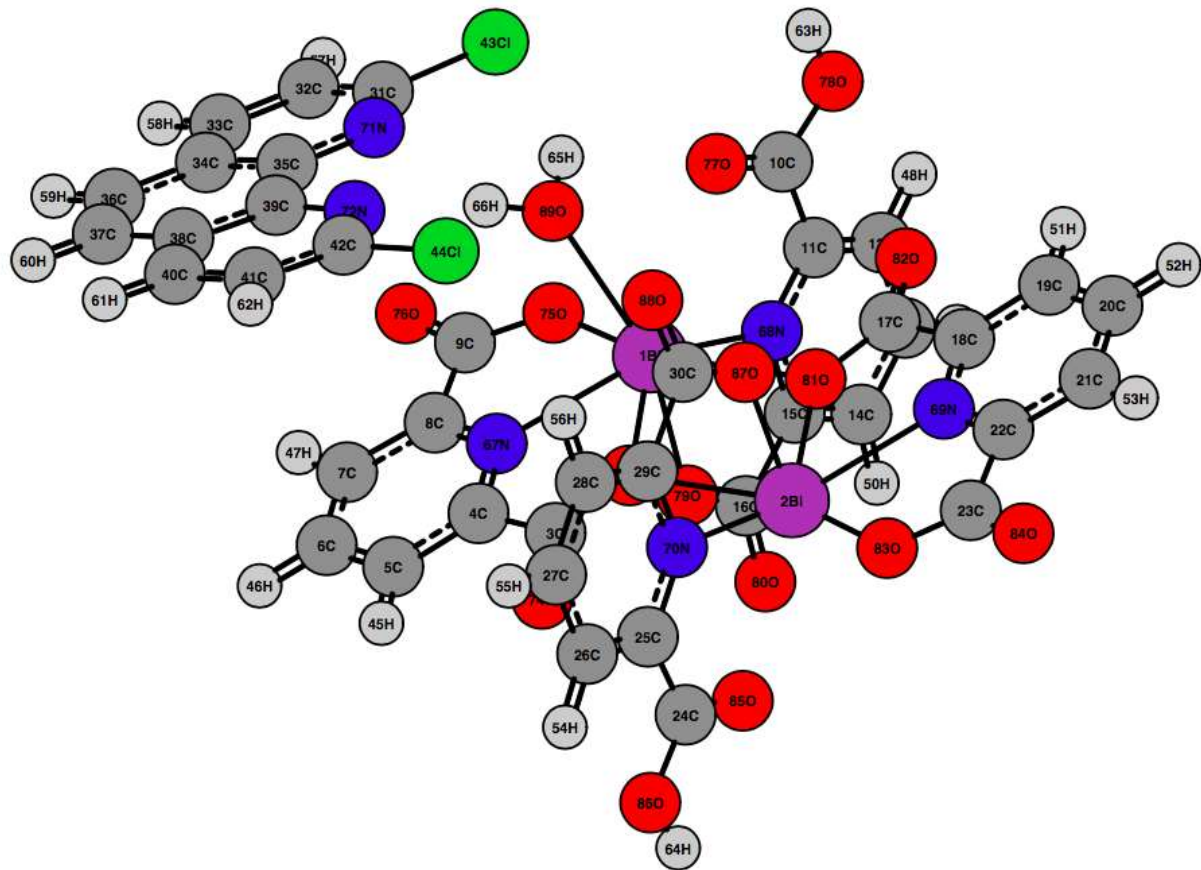


Figure S40. DFT calculated ground state structures for **2**.

Table S7. DFT calculated ground state parameters for **2**.

Bond	Length (Å)	Bond	Length (Å)	Bond	Length (Å)
Bi1 - N67	2.4427	C21 - C20	1.3931	C4 - N67	1.3349
Bi1 - N68	2.5641	C22 - C21	1.3919	C4 - C3	1.5208
Bi1 - O73	2.5630	C22 - N69	1.3342	C40 - C38	1.4136
Bi1 - O75	2.2896	C23 - C22	1.5260	C41 - C40	1.3719
Bi1 - O77	2.8740	C23 - O83	1.3011	C42 - C41	1.4113
Bi1 - O79	2.2478	C23 - O84	1.2158	C42 - Cl4	1.7396
Bi1 - O81	2.6846	C24 - O85	1.2089	C42 - N72	1.3098
Bi1 - O89	2.6588	C24 - O86	1.3393	C5 - C4	1.3916
Bi2 - N69	2.4512	C25 - C24	1.4946	C6 - C5	1.3934
Bi2 - N70	2.5142	C25 - N70	1.3348	C7 - C6	1.3921
Bi2 - O73	2.5989	C26 - C25	1.3893	C8 - N67	1.3333
Bi2 - O81	2.5075	C27 - C26	1.3963	C8 - C7	1.3922
Bi2 - O83	2.2897	C28 - C27	1.3874	C9 - O75	1.2937
Bi2 - O85	2.8667	C29 - C28	1.3960	C9 - O76	1.2208
Bi2 - O87	2.1836	C29 - N70	1.3259	C9 - C8	1.5266
C10 - O77	1.2108	C3 - O73	1.2953		
C10 - O78	1.3386	C3 - O74	1.2249		
C11 - C10	1.4941	C30 - C29	1.5216		
C11 - N68	1.3349	C30 - O87	1.3089		
C12 - C11	1.3902	C30 - O88	1.2134		
C13 - C12	1.3957	C31 - Cl4	1.7485		
C14 - C13	1.3874	C31 - N71	1.3025		
C15 - C14	1.3975	C32 - C31	1.4094		
C15 - N68	1.3283	C33 - C32	1.3711		
C16 - C15	1.5267	C34 - C33	1.4143		
C16 - O79	1.2997	C35 - C34	1.4175		
C16 - O80	1.2161	C35 - N71	1.3525		
C17 - O81	1.2945	C36 - C34	1.4312		
C17 - O82	1.2254	C37 - C36	1.3600		
C18 - C17	1.5212	C38 - C37	1.4298		
C18 - N69	1.3349	C39 - C35	1.4501		
C19 - C18	1.3917	C39 - C38	1.4183		
C20 - C19	1.3932	C39 - N72	1.3565		

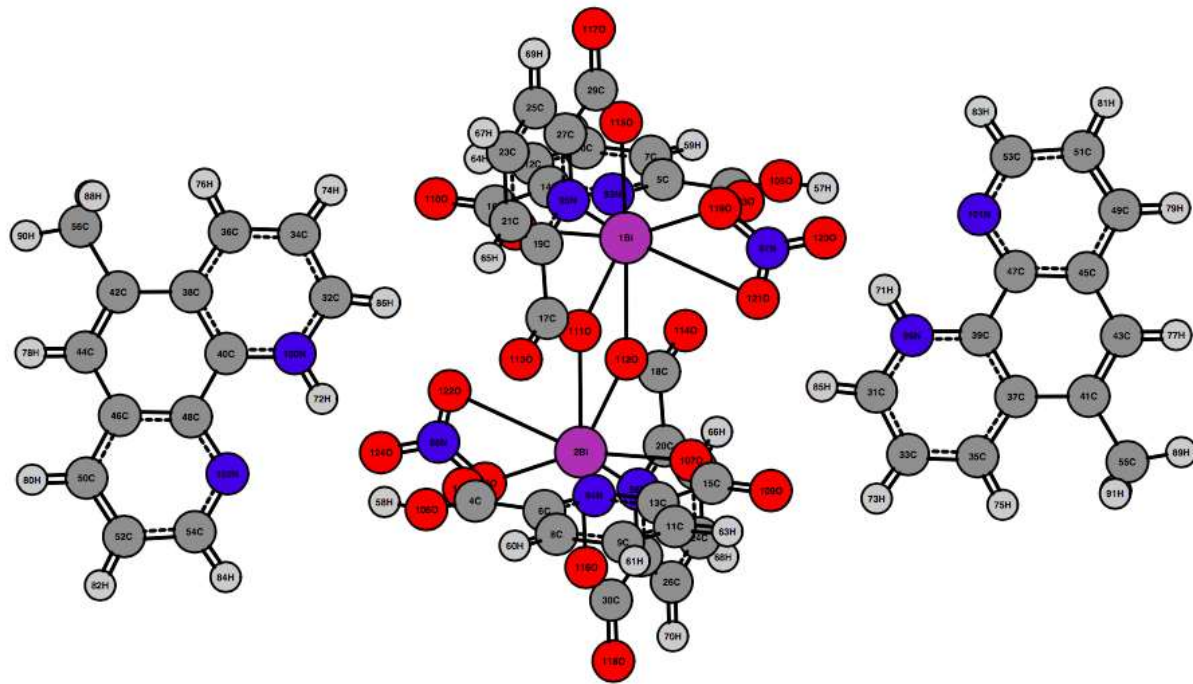


Figure S41. DFT calculated ground state structures for **3**.

Table S8. DFT calculated ground state parameters for **3**.

Bond	Length (Å)	Bond	Length (Å)	Bond	Length (Å)
Bi1 - N93	2.6297	C19 - C17	1.5236	C40 - N100	1.3628
Bi1 - N95	2.4229	C19 - N95	1.3334	C41 - C37	1.4482
Bi1 - O103	2.9111	C20 - C18	1.5236	C42 - C38	1.4478
Bi1 - O108	2.3066	C20 - N96	1.3343	C43 - C41	1.3649
Bi1 - O111	2.5117	C21 - C19	1.3912	C44 - C42	1.3639
Bi1 - O112	2.725	C22 - C20	1.3916	C45 - C43	1.4306
Bi1 - O115	2.2936	C23 - C21	1.3941	C46 - C44	1.4306
Bi1 - O119	2.6534	C24 - C22	1.3942	C47 - C39	1.4411
Bi1 - O121	2.9979	C25 - C23	1.3921	C47 - C45	1.4152
Bi2 - N94	2.625	C26 - C24	1.3921	C47 - N101	1.3466
Bi2 - N96	2.423	C27 - C25	1.3917	C48 - C40	1.44
Bi2 - O104	2.9078	C27 - N95	1.3334	C48 - C46	1.4162
Bi2 - O107	2.3074	C28 - C26	1.3913	C48 - N102	1.3467
Bi2 - O111	2.7244	C28 - N96	1.3325	C49 - C45	1.4124
Bi2 - O112	2.5132	C29 - C27	1.529	C5N - N93	1.3339
Bi2 - O116	2.2945	C29 - O115	1.2948	C5C - C3	1.4957
Bi2 - O120	2.6571	C29 - O117	1.2182	C50 - C46	1.4118
Bi2 - O122	2.9972	C30 - O103	1.2101	C51 - C49	1.3777
C10 - C7	1.3938	C30 - O105	1.3451	C52 - C50	1.3774
C11 - C9	1.3878	C30 - C28	1.5292	C53 - C51	1.4102
C12 - C10	1.3877	C30 - O116	1.2942	C53 - N101	1.3206
C13 - C11	1.397	C30 - O118	1.2192	C54 - C52	1.4105
C13 - N94	1.3268	C31 - N99	1.3311	C54 - N102	1.3194
C14 - C12	1.3981	C32 - N100	1.3308	C55 - C41	1.5088
C14 - N93	1.3258	C33 - C31	1.3969	C56 - C42	1.5073
C15 - C13	1.5232	C34 - C32	1.3976	C6N - N94	1.3337
C15 - O107	1.2826	C35 - C33	1.3776	C6C - C4	1.4931
C15 - O109	1.2318	C36 - C34	1.3778	C7C - C5	1.3908
C16 - C14	1.5235	C37 - C35	1.4145	C8C - C6	1.3918
C16 - O108	1.2825	C38 - C36	1.4157	C9C - C8	1.3946
C16 - O110	1.2312	C39 - C37	1.4138	N97 - O119	1.2581
C17 - O111	1.2908	C39 - N99	1.3624	N97 - O121	1.2512
C17 - O113	1.2257	C40 - O104	1.2083	N97 - O123	1.2567
C18 - O112	1.2908	C40 - O106	1.3437	N98 - O120	1.2562
C18 - O114	1.2257	C40 - C38	1.4131	N98 - O122	1.2523
N98 - O124	1.2565				

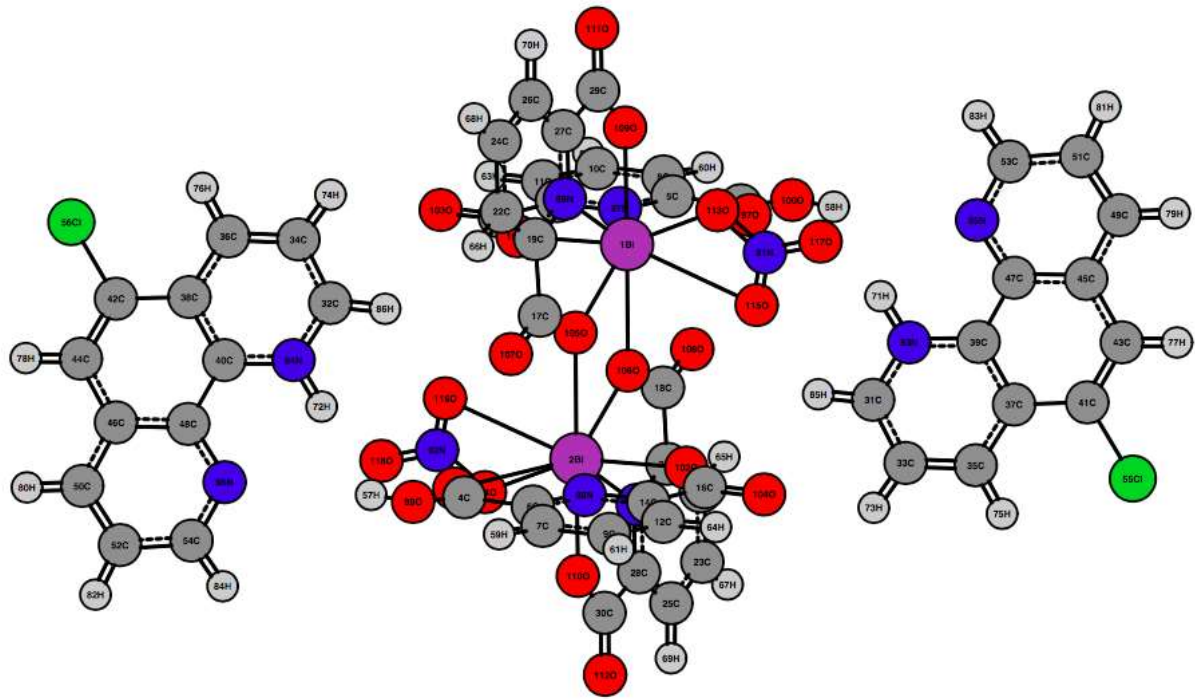


Figure S42. DFT calculated ground state structures for **4**.

Table S9. DFT calculated ground state parameters for **4**.

Bond	Length (Å)	Bond	Length (Å)	Bond	Length (Å)
Bi1 - N87	2.6294	C19 - N89	1.3348	C41 - Cl55	1.7421
Bi1 - N89	2.4216	C20 - C18	1.5237	C42 - C38	1.4419
Bi1 - O101	2.3026	C20 - N90	1.3357	C42 - Cl56	1.7414
Bi1 - O105	2.5098	C21 - C20	1.3919	C43 - C41	1.3611
Bi1 - O106	2.7273	C22 - C19	1.3929	C44 - C42	1.3604
Bi1 - O109	2.2937	C23 - C21	1.3949	C45 - C43	1.4301
Bi1 - O113	2.6702	C24 - C22	1.3947	C46 - C44	1.4309
Bi1 - O115	3.0091	C25 - C23	1.3936	C47 - C39	1.4418
Bi1 - O97	2.9184	C26 - C24	1.3929	C47 - C45	1.4177
Bi2 - N88	2.6302	C27 - C26	1.3937	C47 - N95	1.3458
Bi2 - N90	2.4216	C27 - N89	1.3333	C48 - C40	1.4424
Bi2 - O102	2.3049	C28 - C25	1.3925	C48 - C46	1.4170
Bi2 - O105	2.7290	C28 - N90	1.3338	C48 - N96	1.3467
Bi2 - O106	2.5101	C29 - C27	1.5293	C49 - C45	1.4130
Bi2 - O110	2.2933	C29 - O109	1.2956	C5 - C3	1.4948
Bi2 - O114	2.6702	C29 - O111	1.2199	C5 - N87	1.3340
Bi2 - O116	3.0168	C3 - O100	1.3469	C50 - C46	1.4132
Bi2 - O98	2.9172	C3 - O97	1.2074	C51 - C49	1.3773
C10 - C8	1.3957	C30 - C28	1.5293	C52 - C50	1.3782
C11 - C10	1.3887	C30 - O110	1.2962	C53 - C51	1.4115
C12 - C9	1.3881	C30 - O112	1.2204	C53 - N95	1.3204
C13 - C11	1.3979	C31 - N93	1.3312	C54 - C52	1.4119
C13 - N87	1.3278	C32 - N94	1.3327	C54 - N96	1.3200
C14 - C12	1.3989	C33 - C31	1.3994	C6 - C4	1.4953
C14 - N88	1.3284	C34 - C32	1.3988	C6 - N88	1.3333
C15 - C13	1.5240	C35 - C33	1.3775	C7 - C6	1.3926
C15 - O101	1.2841	C36 - C34	1.3781	C8 - C5	1.3916
C15 - O103	1.2324	C37 - C35	1.4148	C9 - C7	1.3947
C16 - C14	1.5235	C38 - C36	1.4157	N91 - O113	1.2550
C16 - O102	1.2837	C39 - C37	1.4134	N91 - O115	1.2529
C16 - O104	1.2323	C39 - N93	1.3626	N91 - O117	1.2607
C17 - O105	1.2923	C4 - O98	1.2081	N92 - O114	1.2561
C17 - O107	1.2277	C4 - O99	1.3476	N92 - O116	1.2529
C18 - O106	1.2921	C40 - C38	1.4152	N92 - O118	1.2604
C18 - O108	1.2277	C40 - N94	1.3624		
C19 - C17	1.5244	C41 - C37	1.4427		

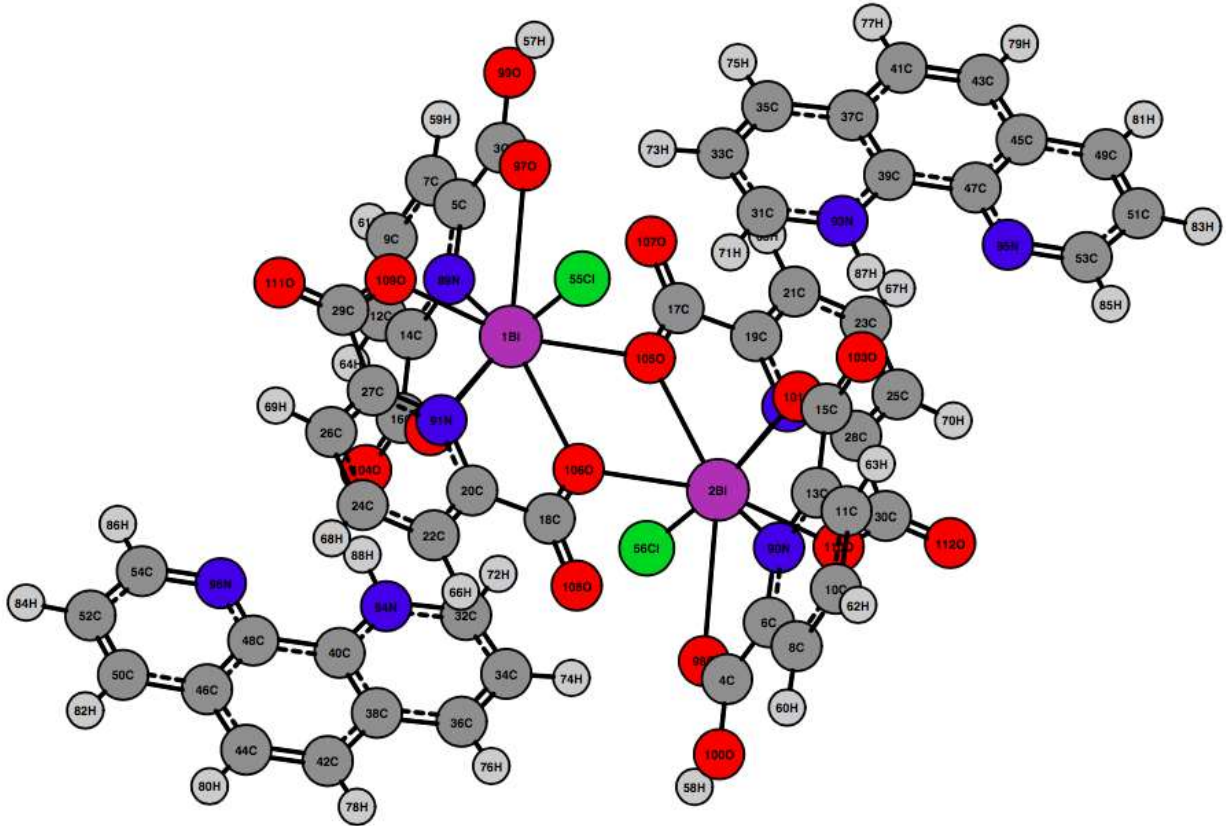


Figure S43. DFT calculated ground state structures for **5**.

Table S10. DFT calculated ground state parameters for **5**.

Bond	Length (Å)	Bond	Length (Å)	Bond	Length (Å)
Bi1 - Cl55	2.6721	C5 - N89	1.3327	C41 - H77	1.0836
Bi1 - N91	2.4009	C7 - C9	1.3928	C43 - C45	1.4327
Bi1 - O109	2.2847	C7 - H59	1.081	C43 - H79	1.0846
C18 - C20	1.5242	C9 - C12	1.3885	C45 - C47	1.419
C18 - O106	1.2859	C9 - H61	1.0838	C45 - C49	1.4118
C18 - O108	1.23	C12 - C14	1.398	C47 - N95	1.3474
C20 - C22	1.3911	C12 - H64	1.0812	C49 - C51	1.3762
C20 - N91	1.3342	C14 - C16	1.5204	C49 - H81	1.0843
C22 - C24	1.3938	C14 - N89	1.3293	C51 - C53	1.4097
C22 - H66	1.0815	C16 - O102	1.2635	C51 - H83	1.0835
C24 - C26	1.3913	C16 - O104	1.2519	C53 - H85	1.0861
C24 - H68	1.0852	H57 - O99	0.9675	C53 - N95	1.3189
C26 - C27	1.3924	C4 - C6	1.4951	H87 - N93	1.0783
C26 - H69	1.0819	C4 - O98	1.2077	C32 - C34	1.397
C27 - C29	1.5274	C4 - O100	1.3479	C32 - H72	1.0833
C27 - N91	1.3319	C6 - C8	1.3931	C32 - N94	1.3305
C29 - O109	1.2947	C6 - N90	1.3332	C34 - C36	1.3766
C29 - O111	1.2188	C8 - C10	1.394	C34 - H74	1.0821
Bi2 - Cl56	2.672	C8 - H60	1.0804	C36 - C38	1.4124
Bi2 - N92	2.401	C10 - C11	1.3889	C36 - H76	1.0845
Bi2 - O110	2.2849	C10 - H62	1.0835	C38 - C40	1.4127
C17 - C19	1.525	C11 - C13	1.3977	C38 - C42	1.4337
C17 - O105	1.2856	C11 - H63	1.0817	C40 - C48	1.4427
C17 - O107	1.2302	C13 - C15	1.5201	C40 - N94	1.3581
C19 - C21	1.3906	C13 - N90	1.3292	C42 - C44	1.3599
C19 - N92	1.3337	C15 - O101	1.2642	C42 - H78	1.0847
C21 - C23	1.3941	C15 - O103	1.252	C44 - C46	1.4331
C21 - H65	1.0807	H58 - O100	0.968	C44 - H80	1.0846
C23 - C25	1.3926	C31 - C33	1.3963	C46 - C48	1.4192
C23 - H67	1.0837	C31 - H71	1.0837	C46 - C50	1.4116
C25 - C28	1.3924	C31 - N93	1.3303	C48 - N96	1.3472
C25 - H70	1.0814	C33 - C35	1.3763	C50 - C52	1.3758
C28 - C30	1.528	C33 - H73	1.0825	C50 - H82	1.0857
C28 - N92	1.3329	C35 - C37	1.413	C52 - C54	1.4103
C30 - O110	1.2947	C35 - H75	1.084	C52 - H84	1.0833
C30 - O112	1.2187	C37 - C39	1.4119	C54 - H86	1.0863
C3 - C5	1.4943	C37 - C41	1.4345	C54 - N96	1.3194
C3 - O97	1.2081	C39 - C47	1.4424	H88 - N94	1.0782
C3 - O99	1.3474	C39 - N93	1.3581		
C5 - C7	1.3939	C41 - C43	1.3596		

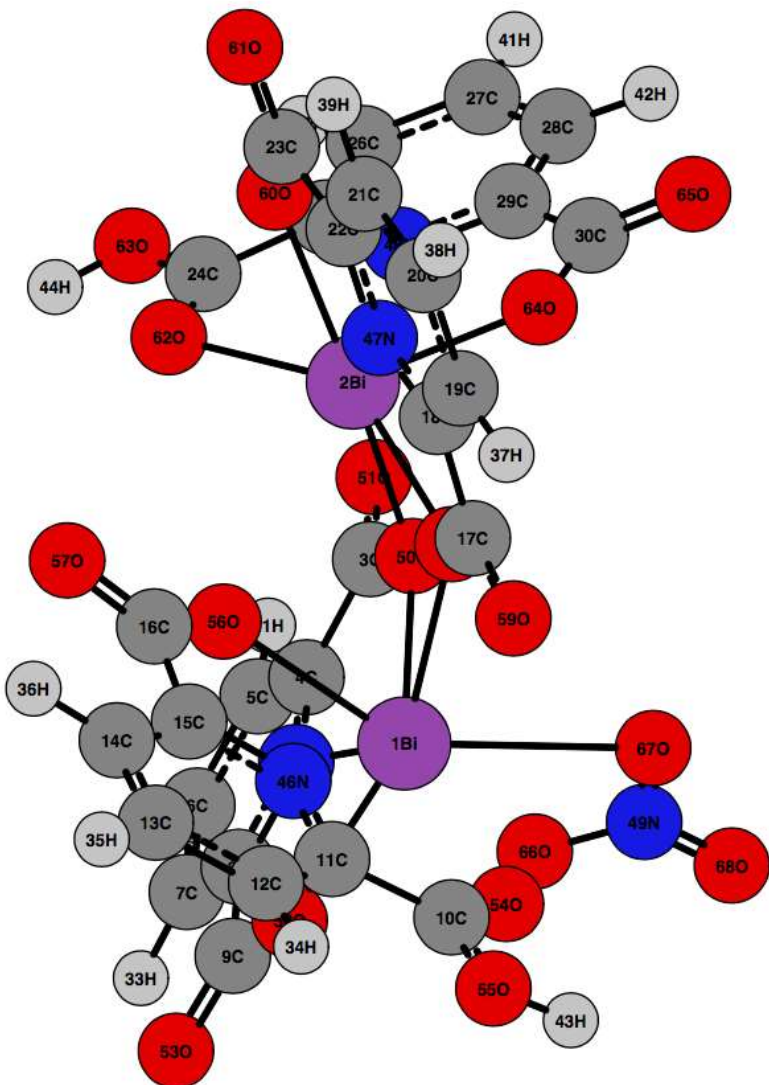


Figure S44. DFT calculated optimized *singlet* state parameters for the anionic $[\text{Bi}_2(\text{HPDC})_2(\text{PDC})_2(\text{NO}_3)]^-$ dimeric unit found in **1**.

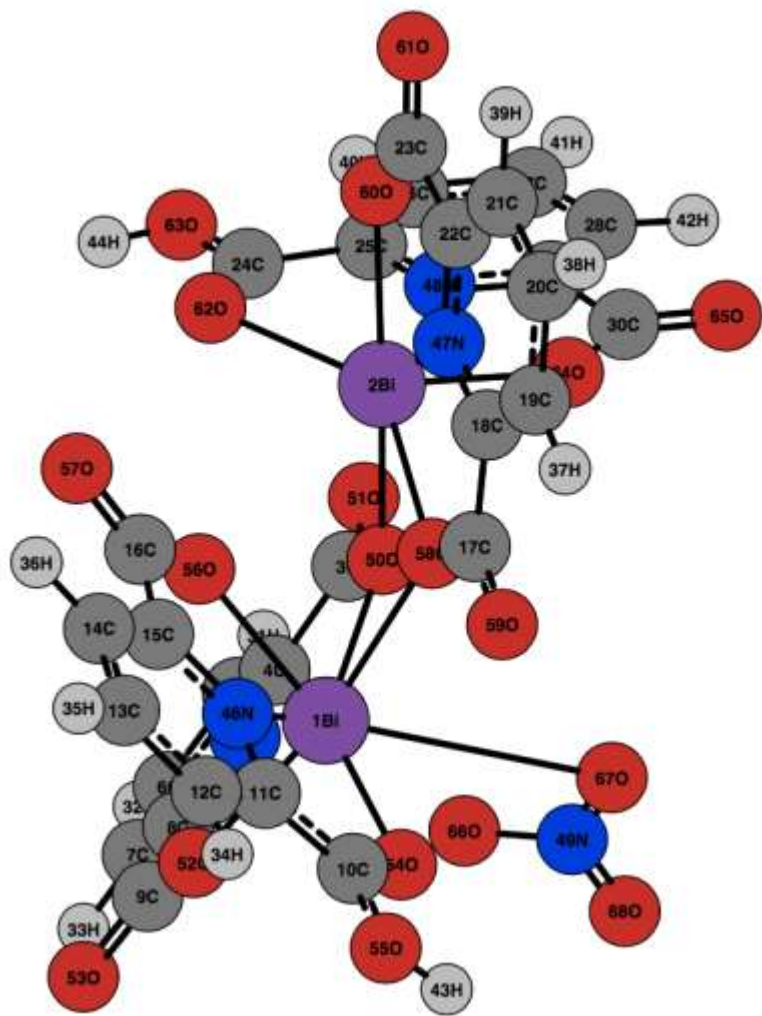


Figure S45. DFT calculated optimized *doublet* state parameters for the neutral $[\text{Bi}_2(\text{HPDC})_2(\text{PDC})_2(\text{NO}_3)]^0$ dimeric unit found in **1**.

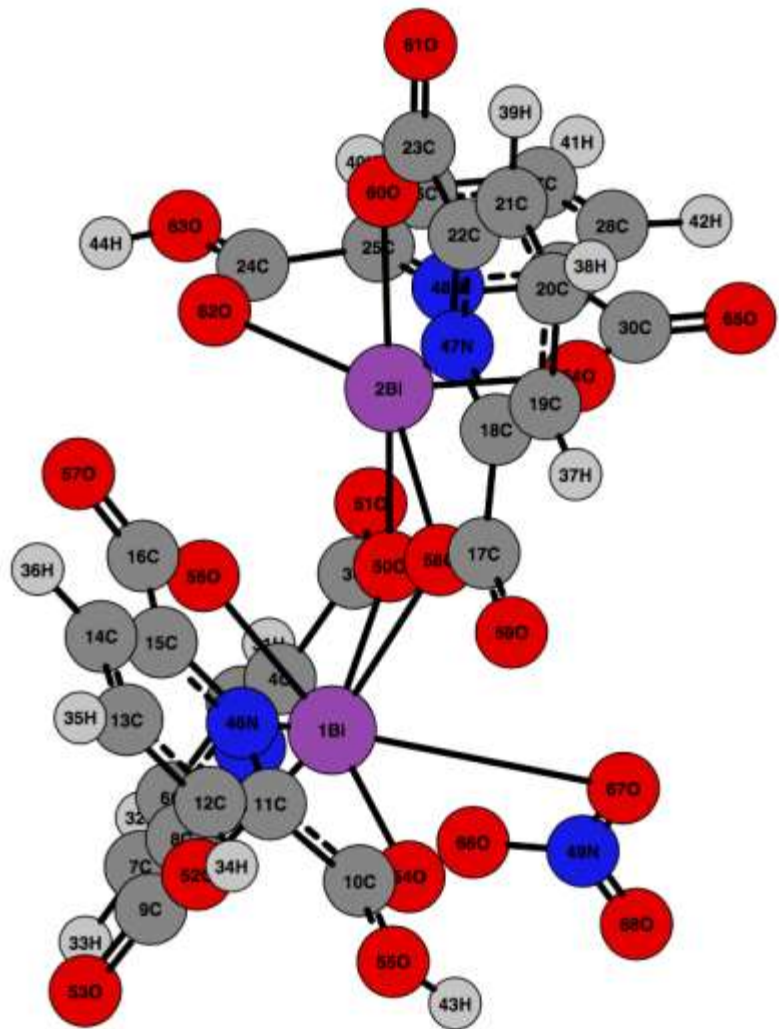


Figure S46. DFT calculated optimized *triplet* state parameters for the anionic $[\text{Bi}_2(\text{HPDC})_2(\text{PDC})_2(\text{NO}_3)]^-$ dimeric unit found in **1**.

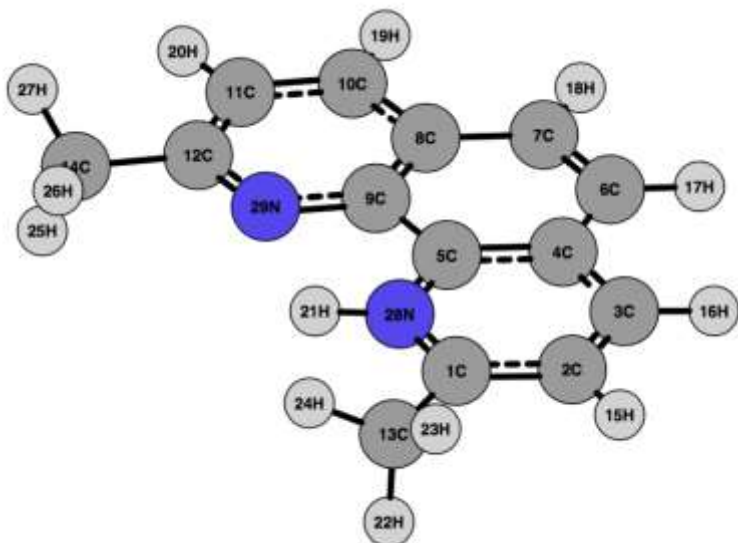


Figure S47. DFT calculated optimized *singlet* state parameters for the organic cationic $[\text{PhenH}]^{+1}$ unit found in **1**.

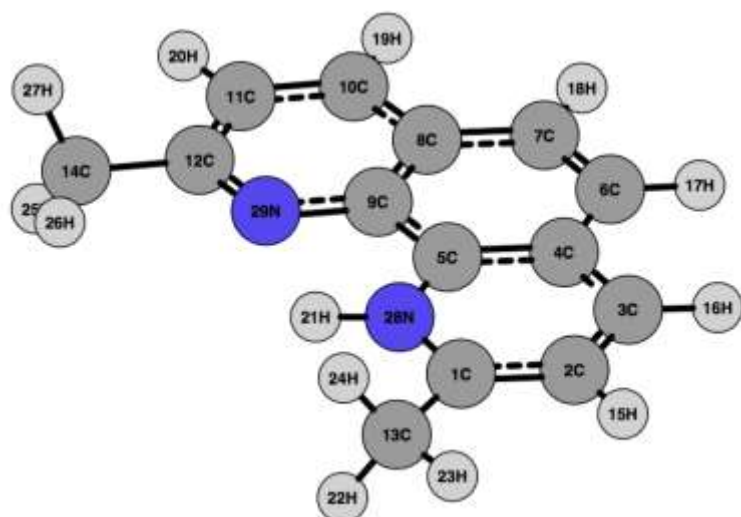


Figure S48. DFT calculated optimized *doublet* state parameters for the organic neutral $[\text{PhenH}]^0$ unit found in **1**.

Table S11. Calculated frontier molecular orbital energies for **1-5**.

	1	2	3	4	5
HOMO (eV)	-6.52	-6.61	-5.85	-5.94	-5.93
LUMO (eV)	-2.96	-2.46	-2.86	-3.06	-2.72
Bandgap (eV)	3.56	4.16	2.99	2.88	3.21

Table S12. TD-DFT calculated parameters and transitions for the lowest bright excited *singlet* state of **1-5** with f-oscillator strength >0.01.

Compound	Donor MO		Acceptor MO	Coeff.	% Coeff.	λ	Energy	f-Oscillator Strength	
1	252	HOMO-11	→ 264	LUMO	0.43894	40%	330.3 nm	3.7536 eV	0.0163
	251	HOMO-12	→ 264	LUMO	0.34778	25%			
	253	HOMO-10	→ 264	LUMO	-0.28598	17%			
	255	HOMO-8	→ 264	LUMO	-0.27202	15%			
	246	HOMO-17	→ 265	LUMO+1	-0.10838	2%			
2	256	HOMO-4	→ 264	LUMO+3	0.36066	29%	302.3 nm	4.1018 eV	0.0204
	252	HOMO-8	→ 262	LUMO+1	0.32791	24%			
	257	HOMO-3	→ 264	LUMO+3	-0.31419	22%			
	256	HOMO-4	→ 261	LUMO	-0.18051	7%			
	256	HOMO-4	→ 262	LUMO+1	-0.14985	5%			
	250	HOMO-10	→ 262	LUMO+1	0.11448	3%			
	258	HOMO-2	→ 262	LUMO+1	-0.11149	3%			
	260	HOMO	→ 264	LUMO+3	0.10891	3%			
	259	HOMO-1	→ 262	LUMO+1	-0.10887	3%			
	251	HOMO-9	→ 262	LUMO+1	-0.10078	2%			
3	306	HOMO-20	→ 328	LUMO+1	0.54465	68%	328.1 nm	3.7784 eV	0.0207
	311	HOMO-15	→ 328	LUMO+1	-0.21074	10%			
	305	HOMO-21	→ 327	LUMO	-0.17009	7%			
	296	HOMO-30	→ 330	LUMO+3	0.13855	4%			
	310	HOMO-16	→ 328	LUMO+1	-0.13532	4%			
	312	HOMO-14	→ 328	LUMO+1	-0.12477	4%			
	309	HOMO-17	→ 328	LUMO+1	0.11668	3%			
4	312	HOMO-22	→ 335	LUMO	0.36839	31%	331.4 nm	3.7407 eV	0.0106
	323	HOMO-11	→ 337	LUMO+2	-0.34415	27%			
	313	HOMO-21	→ 335	LUMO	-0.33979	26%			
	317	HOMO-17	→ 335	LUMO	0.18315	8%			
	314	HOMO-20	→ 335	LUMO	-0.13335	4%			
	302	HOMO-32	→ 337	LUMO+2	0.12642	4%			
5	283	HOMO-21	→ 306	LUMO+1	0.24241	18%	288.0 nm	4.3046 eV	0.0146
	286	HOMO-18	→ 306	LUMO+1	-0.22177	15%			
	283	HOMO-21	→ 305	LUMO	0.20012	12%			
	282	HOMO-22	→ 306	LUMO+1	0.18693	11%			
	282	HOMO-22	→ 305	LUMO	0.15772	8%			
	272	HOMO-32	→ 307	LUMO+2	0.15264	7%			
	291	HOMO-13	→ 307	LUMO+2	0.13975	6%			
	286	HOMO-18	→ 307	LUMO+2	-0.13018	5%			
	286	HOMO-18	→ 305	LUMO	0.12727	5%			

291	HOMO-13	→	308	LUMO+3	0.12047	5%
295	HOMO-9	→	309	LUMO+4	-0.11286	4%
273	HOMO-31	→	308	LUMO+3	-0.10387	3%

Table S13. TD-DFT calculated parameters and transitions for the lowest excited *singlet* state of **1–5** with f-oscillator strength <0.01.

Compound	Donor MO		Acceptor MO		Coeff.	% Coeff.	λ	Energy	f-Oscillator Strength	
1	262	HOMO-1	→	264	LUMO	0.66799	91%	414.2 nm	2.9931 eV	0.0013
	263	HOMO	→	264	LUMO	0.21515	8%			
2	259	HOMO-1	→	261	LUMO	-0.15334	5%	342.6 nm	3.6191 eV	0.0039
	260	HOMO	→	261	LUMO	0.66743	95%			
3	326	HOMO	→	327	LUMO	0.69768	100%	467.8 nm	2.6503 eV	0.0001
4	334	HOMO	→	335	LUMO	0.69926	100%	486.1 nm	2.5507 eV	0.0001
5	304	HOMO	→	305	LUMO	0.70148	100%	450.8 nm	2.7501 eV	0.0003

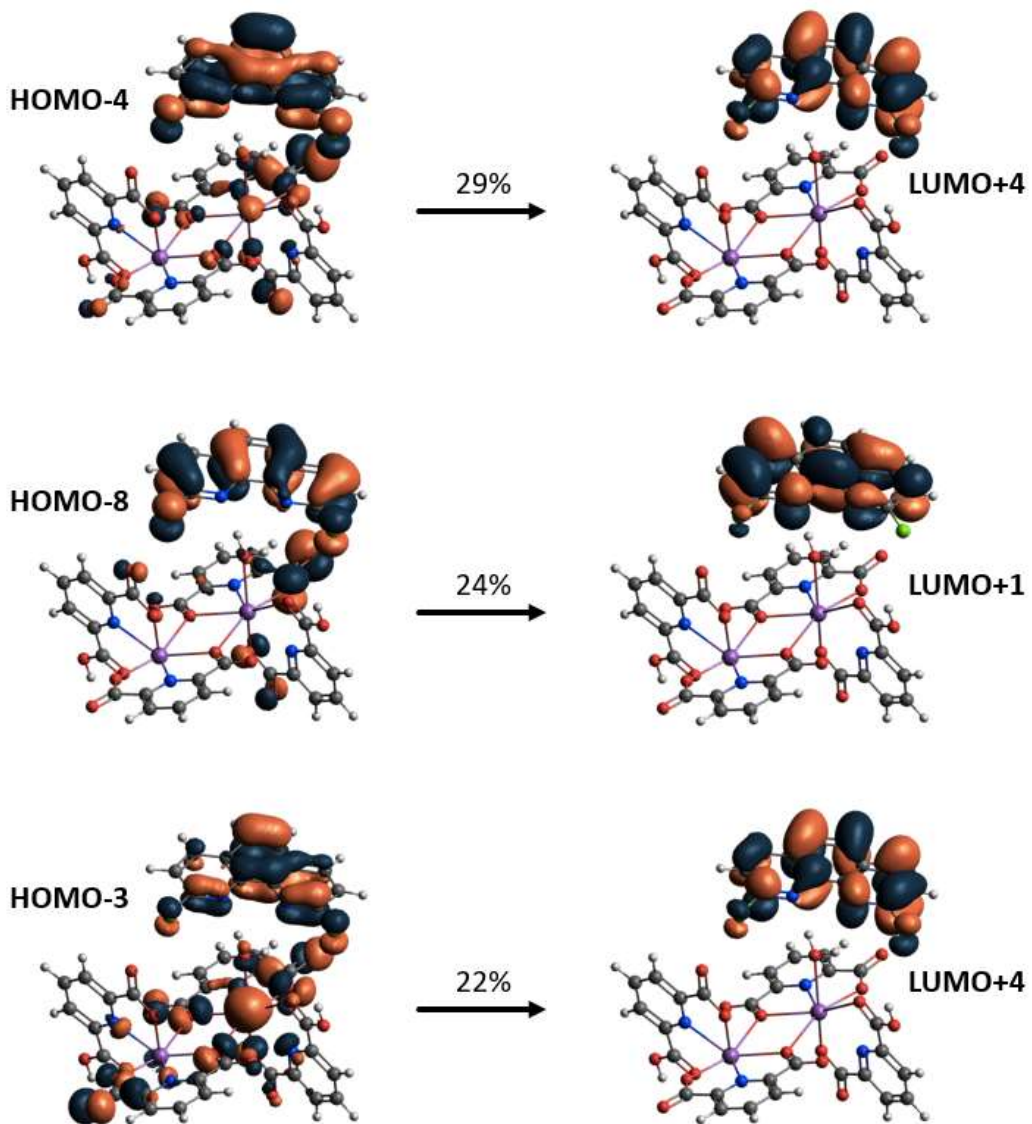


Figure S49. TD-DFT calculated dominant orbital transitions for the lowest excited *singlet* state of **2**.

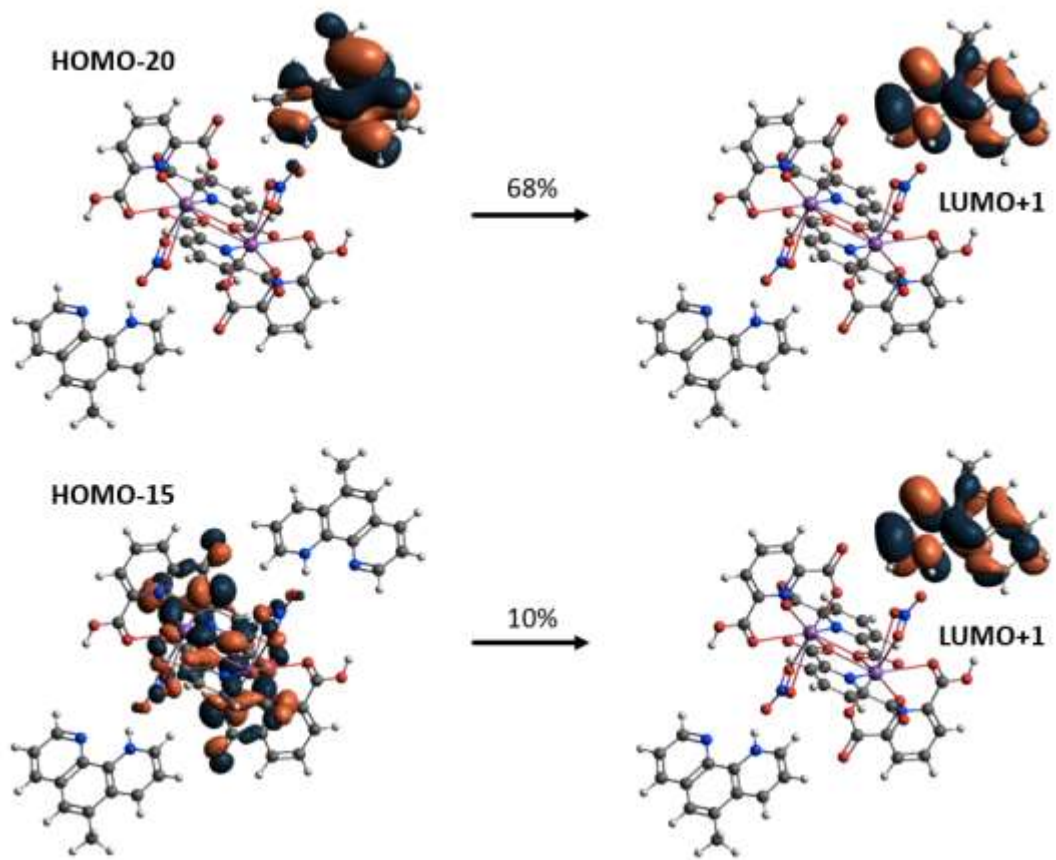


Figure S50. TD-DFT calculated dominant orbital transitions for the lowest excited *singlet* state of **3**.

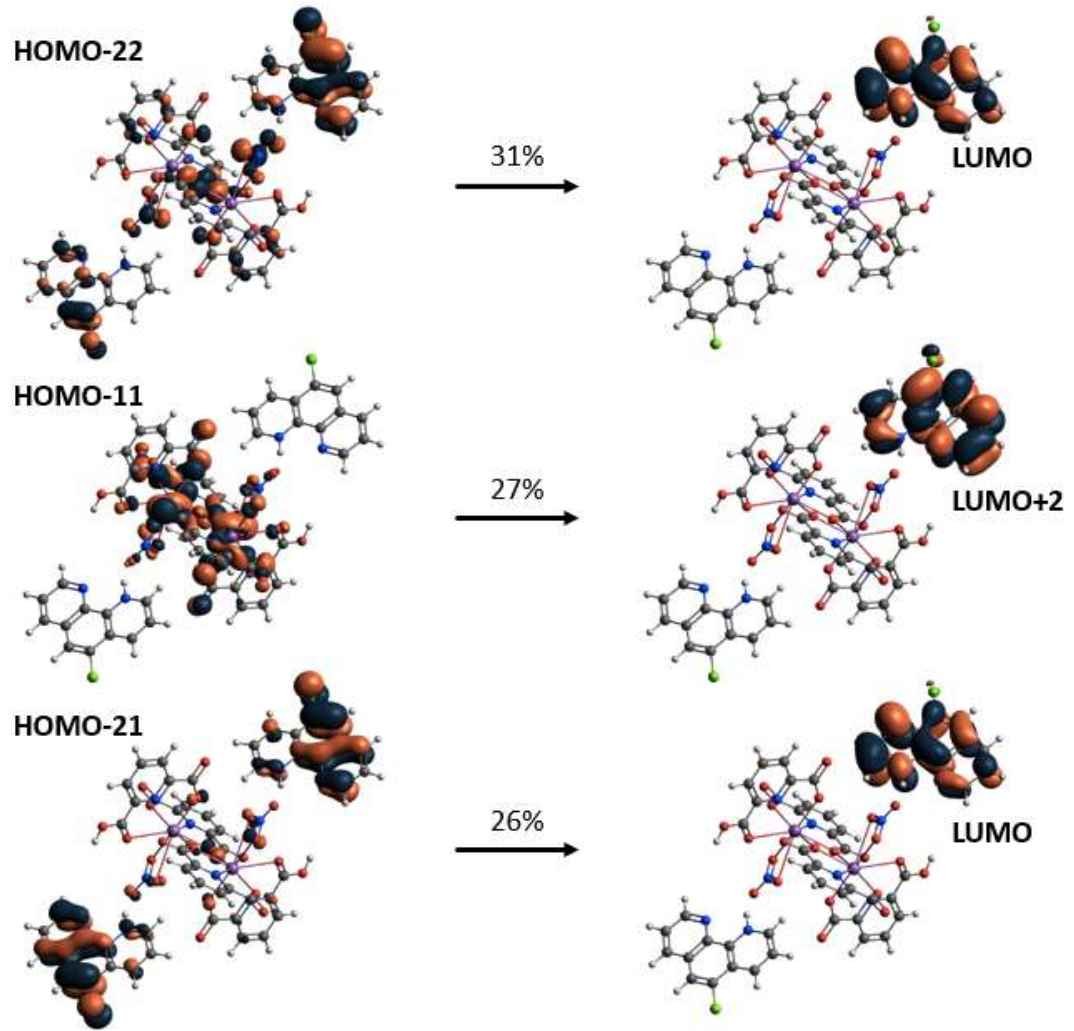


Figure S51. TD-DFT calculated dominant orbital transitions for the lowest excited *singlet* state of **4**.

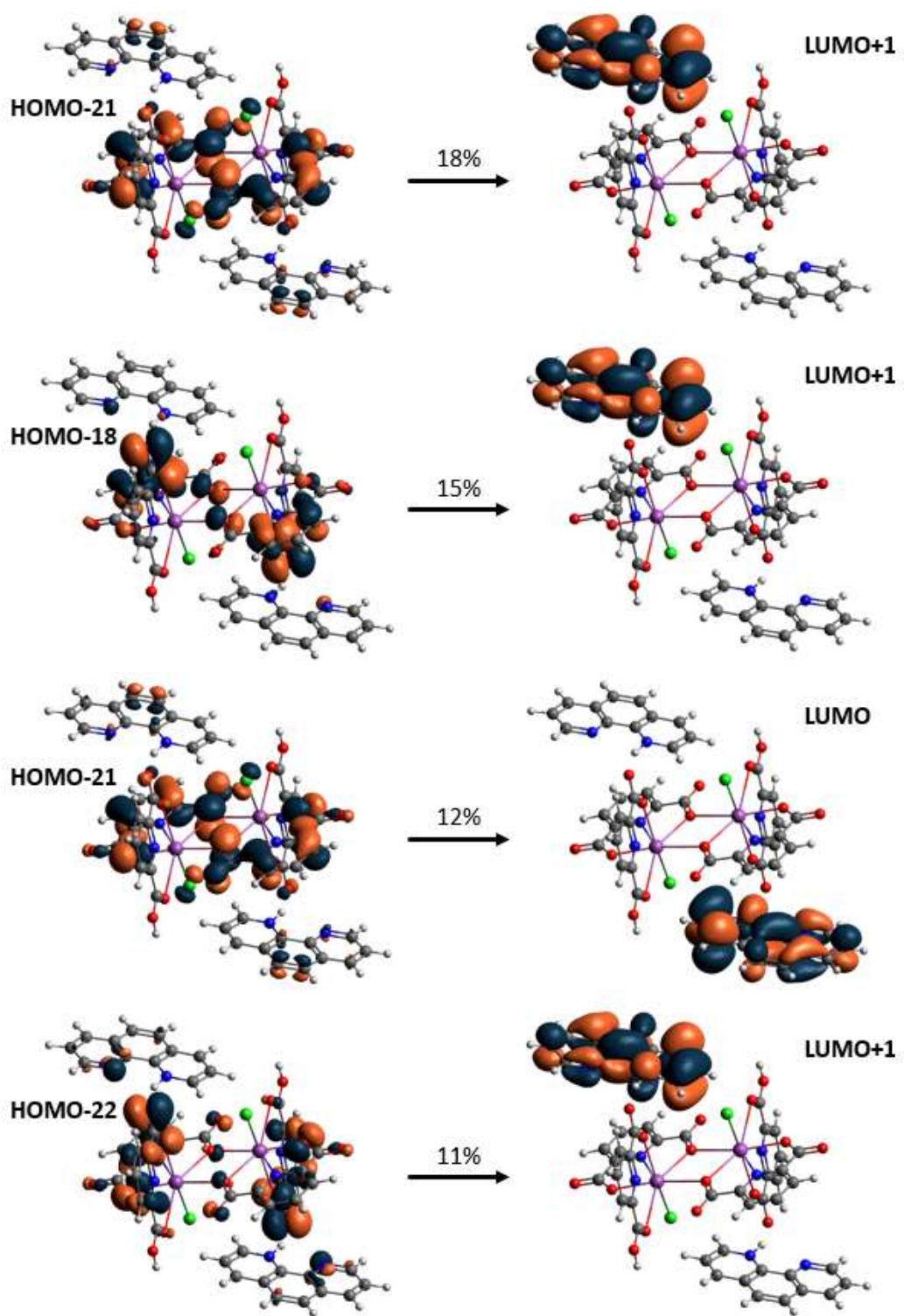


Figure S52. TD-DFT calculated dominant orbital transitions for the lowest excited *singlet* state of **5**.

Table S14. TD-DFT calculated parameters and transitions for the lowest excited *triplet* state of **1-5**.

Compound	Donor MO		Acceptor MO		Coeff.	% Coeff.	λ	Energy
1	252	HOMO-11	→	264	LUMO	0.29524	21%	2.8755 eV
	253	HOMO-10	→	264	LUMO	-0.25879	16%	
	252	HOMO-11	→	265	LUMO+1	-0.25333	15%	
	253	HOMO-10	→	265	LUMO+1	0.23331	13%	
	251	HOMO-12	→	264	LUMO	0.15899	6%	
	246	HOMO-17	→	264	LUMO	-0.15802	6%	
	262	HOMO-1	→	264	LUMO	0.15483	6%	
	246	HOMO-17	→	265	LUMO+1	-0.13919	5%	
	254	HOMO-9	→	265	LUMO+1	-0.13545	4%	
	254	HOMO-9	→	264	LUMO	0.13518	4%	
	224	HOMO-9	→	264	LUMO	0.10927	3%	
2	256	HOMO-4	→	264	LUMO+3	0.38399	39%	2.8491 eV
	257	HOMO_3	→	264	LUMO+3	-0.30207	24%	
	257	HOMO_3	→	262	LUMO+1	0.20287	11%	
	256	HOMO-4	→	262	LUMO+1	-0.20042	11%	
	252	HOMO-8	→	262	LUMO+1	0.16813	7%	
	252	HOMO-8	→	264	LUMO+3	0.13633	5%	
	258	HOMO-2	→	264	LUMO+3	0.11701	4%	
3	326	HOMO	→	327	LUMO	0.69645	100%	2.6497 eV
4	334	HOMO	→	335	LUMO	0.69887	100%	2.5504 eV
5	304	HOMO	→	305	LUMO	0.67095	91%	2.7460 eV
	304	HOMO	→	306	LUMO+1	-0.20190	8%	451.1 nm

Table S15. Total energies of BiPDC and phen units in **1-5**. The values are obtained from optimized isolated units.

Compound	Species	Charge	Unpaired e ⁻	Multiplicity	Energy (Ht)	Energy (kJ/mol)
1	Bi	-1	0	1	-3208.90917042	-8424991.027
	Phen	1	0	1	-650.80984030	-1708701.236
	Bi*	-1	2	3	-3208.80529920	-8424718.313
	Bi	0	1	2	-3208.72854770	-8424516.802
	Phen	0	1	2	-650.98798690	-1709168.960
2	Bi	0	0	1	-3004.89459321	-7889350.754
	Phen	0	0	1	-1490.99700136	-3914612.627
	Bi*	0	2	3	-3004.77917547	-7889047.725
	Bi	-1	1	2	-3004.97043771	-7889549.879
	Phen	1	1	2	-1491.02498663	-3914686.102
3	Bi	-1	0	1	-3489.31443710	-9161195.055
	Phen	1	0	1	-611.46875741	-1605411.223
	Bi*	-1	2	3	-3489.21213351	-9160926.457
	Bi	0	1	2	-3489.22179970	-9160937.372
	Phen	0	1	2	-611.65324789	-1605895.602
4	Bi	-1	0	1	-3489.31500787	-9161196.553
	Phen	1	0	1	-1031.75710244	-2708878.272
	Bi*	-1	2	3	-3489.21020063	-9160921.382
	Bi	0	1	2	-3489.21973812	-9160941.107
	Phen	0	1	2	-1031.95002118	-2709384.781
5	Bi	-1	0	1	-3849.05678829	-10105698.598
	Phen	1	0	1	-572.13919661	-1502151.461
	Bi*	-1	2	3	-3848.95847985	-10105440.489
	Bi	0	1	2	-3848.97119595	-10105474.749
	Phen	0	1	2	-572.32574140	-1502641.234

Table S16. Change in Gibbs free energy for the proposed transfer of an electron from the donor BiHPDC to the organic acceptor R-PhenH units in **1-5**.

Reaction			ΔG (kJ/mol)
1	Step 1	$^1[Bi]^n + ^1[HXPhen]^m + h\nu \rightarrow ^3[Bi]^n + ^1[HXPhen]^m$	+273
	Step 2	$^3[Bi]^n + ^1[HXPhen]^m \rightarrow ^2[Bi]^{n+1} + ^2[HXPhen]^{m-1}$	+6.5
2	Step 1	$^1[Bi]^n + ^1[HXPhen]^m + h\nu \rightarrow ^3[Bi]^n + ^1[HXPhen]^m$	+303
	Step 2	$^3[Bi]^n + ^1[HXPhen]^m \rightarrow ^2[Bi]^{n+1} + ^2[HXPhen]^{m-1}$	-273
3	Step 1	$^1[Bi]^n + ^1[HXPhen]^m + h\nu \rightarrow ^3[Bi]^n + ^1[HXPhen]^m$	+267
	Step 2	$^3[Bi]^n + ^1[HXPhen]^m \rightarrow ^2[Bi]^{n+1} + ^2[HXPhen]^{m-1}$	-241
4	Step 1	$^1[Bi]^n + ^1[HXPhen]^m + h\nu \rightarrow ^3[Bi]^n + ^1[HXPhen]^m$	+275
	Step 2	$^3[Bi]^n + ^1[HXPhen]^m \rightarrow ^2[Bi]^{n+1} + ^2[HXPhen]^{m-1}$	-256
5	Step 1	$^1[Bi]^n + ^1[HXPhen]^m + h\nu \rightarrow ^3[Bi]^n + ^1[HXPhen]^m$	+258
	Step 2	$^3[Bi]^n + ^1[HXPhen]^m \rightarrow ^2[Bi]^{n+1} + ^2[HXPhen]^{m-1}$	-265

Table S17. Rhem-Weller analysis parameters for **1-5**.

Compound	E_{ox}	E_{red}	E_s	ϵ_o^2/ϵ^a	ΔG_{ET}	
1	-4.91 eV	4.85 eV	385 nm	3.22 eV	0.15 eV	-12.71 eV
2	2.06 eV	0.76 eV	365 nm	3.40 eV	0.06 eV	-1.95 eV
3	-2.67 eV	5.02 eV	403 nm	3.08 eV	0.15 eV	-10.64 eV
4	-2.65 eV	5.25 eV	391 nm	3.17 eV	0.15 eV	-10.77 eV
5	-2.32 eV	5.08 eV	403 nm	3.08 eV	0.15 eV	-10.27 eV

X. Additional Excitation and Emission Spectra

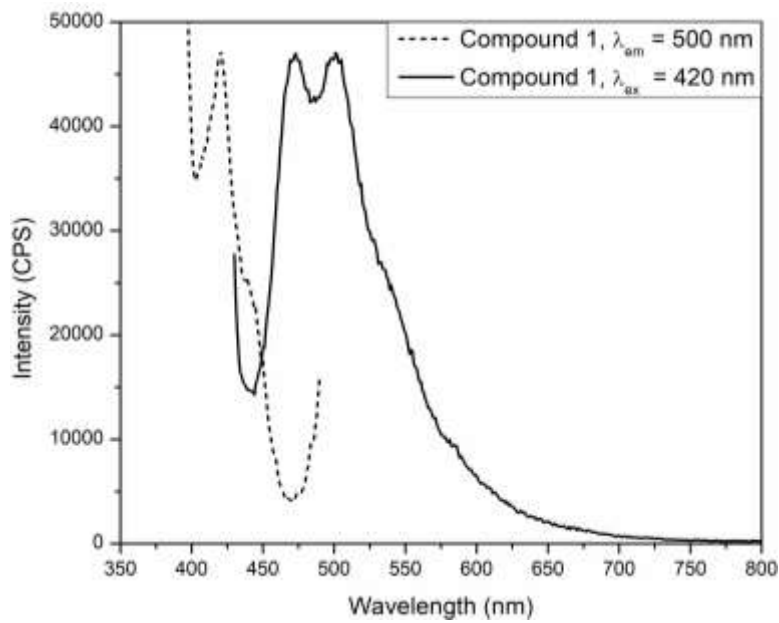


Figure S53. Excitation spectra of **1** ($\lambda_{\text{em}} = 500 \text{ nm}$; dashed line) observed from 350 to 490 nm, highlighting the visible excitation peak at 420 nm, and the emission spectra upon excitation at 420 nm (solid line). The intensity is < 5% of the intensity observed at the maximum excitation wavelength (380 nm).

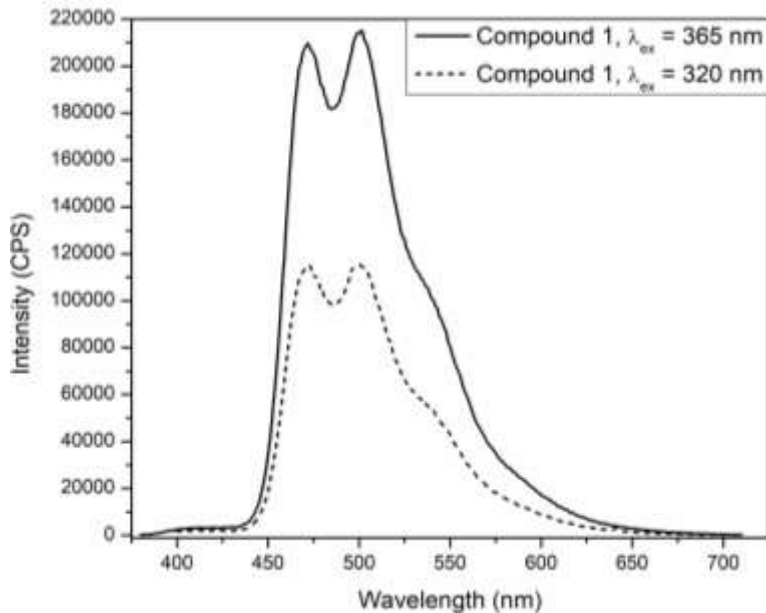


Figure S54. Emission spectra of **1** upon excitation at 320 nm (dashed line) and 365 nm (solid line). These wavelengths were observed as less intense local maxima in the excitation spectrum of **1** (Figure 7). The profile is identical to that previously observed.

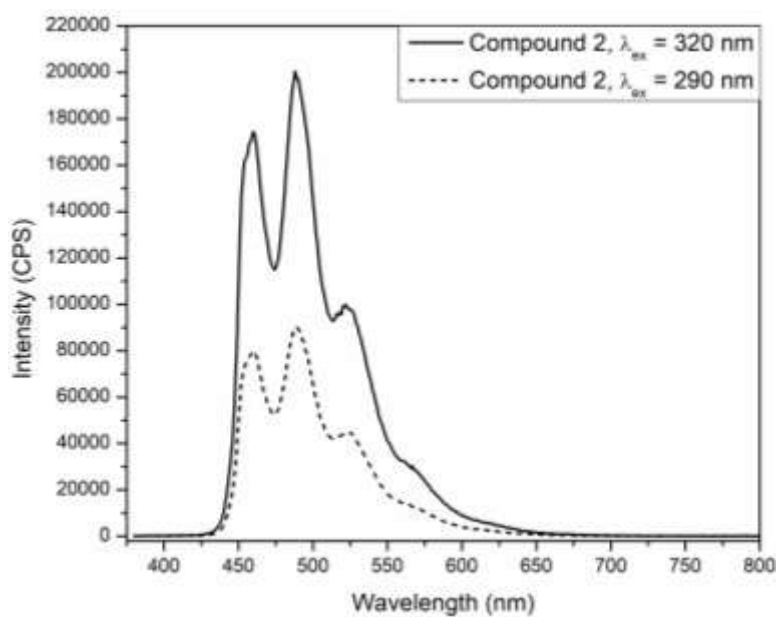


Figure S55. Emission spectra of **2** upon excitation at 290 nm (dashed line) and 320 nm (solid line). These wavelengths were observed as less intense local maxima in the excitation spectrum of **2** (Figure 7). The profile is identical to that previously observed.